Journal of Experimental Psychology:
Human Perception and Performance
2002, Vol. 28, No. 5, 1100–1119

0096-1523/02/$5.00 DOI: 10.1037//0096-1523.28.5.1100

Perceiving Curvilinear Heading in the Presence of Moving Objects

Brett R. Fajen and Nam-Gyoon Kim
University of Connecticut

Four experiments were directed at understanding the influence of multiple moving objects on curvilinear (i.e., circular and elliptical) heading perception. Displays simulated observer movement over a ground plane in the presence of moving objects depicted as transparent, opaque, or black cubes. Objects either moved parallel to or intersected the observer's path and either retreated from or approached the moving observer. Heading judgments were accurate and consistent across all conditions. The significance of these results for computational models of heading perception and for information in the global optic flow field about observer and object motion is discussed.

Locomotion is an integral part of many of the basic activities that humans and other animals routinely perform. For creatures with eyes, changing patterns of light distributions, commonly referred to as *optical flow*, are the primary basis for guidance of locomotion. In the ideal case, the optical flow resulting from linear observer translation parallel to a vacant ground surface can be characterized as a "melon-shaped family of curves" (Gibson, 1966, 1979/1986) with a singularity, the *focus of expansion* (FOE), corresponding to the direction of locomotion (Figure 1A). In steering on a straight path toward an object, one needs only to keep this singularity coincident with the object. Often, however, environments contain objects that move independently of the observer, a situation people encounter on a daily basis when driving through traffic or walking along a crowded sidewalk. The presence of independently moving objects guarantees that the optical flow available to a moving observer will deviate from the ideal case described above (Figure 1B). Yet, we safely navigate through such environments with ease and regularity. A central question, therefore, is the following: What is the form of the information contained in optical distributions that subserves the control of locomotion through environments containing moving objects?

Computational Approaches to Heading Perception

A number of computational models have been proposed to characterize the formal aspects of retinal flow resulting from observer translation with concomitant eye rotation (Bruss & Horn, 1983; Heeger & Jepson, 1990; Hildreth, 1992; Longuet-Higgins & Prazdny, 1980; Perrone, 1992; Rieger & Lawton, 1985; see Warren, 1995, for a review). Retinal flow, namely, the change in the retinal image, can be induced by any relative motion between the point of observation and objects in the environment. Assuming that the environment is stationary without any independently moving objects, one can ascribe any change in the retinal image solely to the combination of observer translation and eye rotation. That is, retinal flow is uniquely determined by the observer's translational velocity, denoted as (v_x, v_y, v_z) and rotational velocity, denoted as $(\omega_x, \omega_y, \omega_z)$ (see Longuet-Higgins & Prazdny, 1980, for further details). According to this view, optical flow (the transformation in optical structure due to observer translation) contains the relevant information for observer movement, namely the FOE, but retinal flow (the transformation in retinal structure due to both observer translation and eye rotation) does not (cf. Cutting, 1986; Cutting, Springer, Braren, & Johnson, 1992). Perceiving heading from retinal flow requires that the observer extract the translational component of optical flow (i.e., the radial pattern of expansion or the FOE).

From a computational perspective, it is generally assumed that the measurement of image motion by biological systems cannot be infinitely precise. Accordingly, any adequate computational procedure must be sufficiently robust to tolerate noise inherent in the measured flow field before extracting the motion parameters from the retinal flow. Of the computational models designed specifically to handle noise, two approaches are notable.

The first approach capitalizes on the fact that a unique image pattern arises during linear translation; that is, all image vectors radiate from a single point, the FOE. For example, least squares models (Bruss & Horn, 1983) search the space of possible motion parameters and iteratively reduce the difference between corresponding and observed patterns until the motion parameters are found that best account for the global flow pattern (see also Ballard & Kimball, 1983; Heeger & Jepson, 1992; Prazdny, 1981). The model exploits redundancy in the flow field by sampling many image points and is therefore quite robust. This approach has also been implemented as a set of neural templates (or template models). For example, one template model, based on the properties of neural cells found in the middle temporal and medial superior temporal areas of the primate visual cortex, postulates sets of sensors and detectors (e.g., Hatsopoulos & Warren, 1990; Perrone,

Brett R. Fajen and Nam-Gyoon Kim, Center for the Ecological Study of Perception and Action, University of Connecticut.

Nam-Gyoon Kim is now at the Department of Psychology, William Paterson University.

We thank Michael T. Turvey for many helpful discussions and comments on a previous version of this article, Judith A. Effken for careful reading of earlier versions, and an anonymous reviewer for helpful criticism.

Correspondence concerning this article should be addressed to Brett R. Fajen, who is now at the Department of Cognitive Science, Rensselaer Polytechnic Institute, Carnegie 305, 110 8th Street, Troy, New York 12180. E-mail: fajenb@rpi.edu

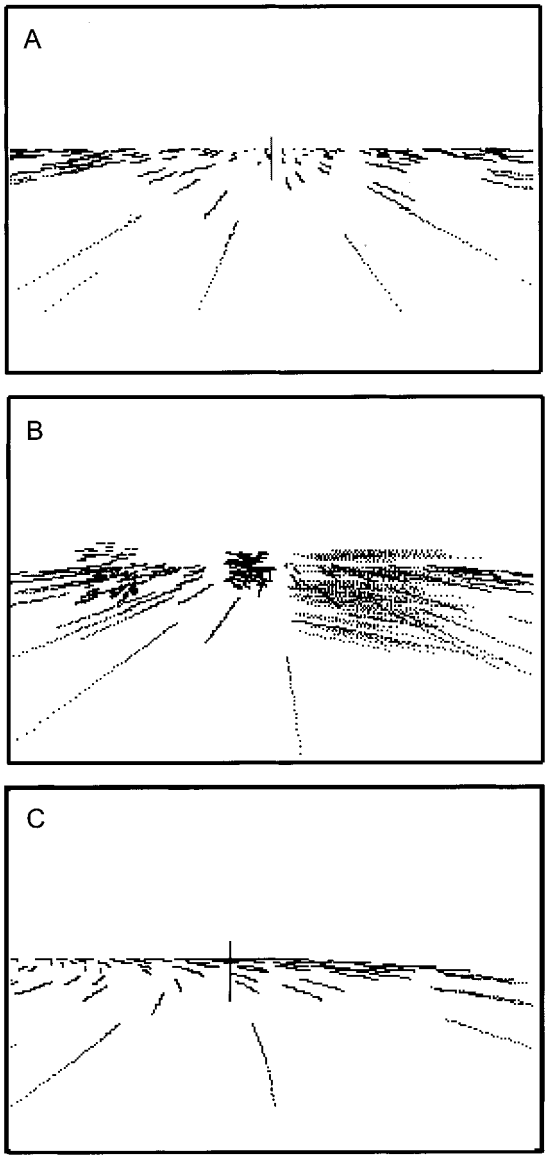

Figure 1. Flow fields corresponding to an observer's movement along a linear path (A), along a linear path in the presence of moving objects (B), and along a circular path (C), parallel to a ground plane. In A and B, the observer's direction of heading is specified by the singularity of the flow field (i.e., the focus of expansion). In C, such a singularity is absent.

1992; Perrone & Stone, 1994; Warren & Saunders, 1995). Sensors populating the entire visual field are tuned to a specific direction and motion velocity. Sensor outputs are then fed into detectors where the signal is integrated. The detector with the largest output identifies direction of heading. In a sense, each detector becomes a template for a specific global pattern. Because all image velocity vectors enter the computation, the influence of measurement error is reduced, allowing these models to tolerate noise.

The second approach to handling noise is based on the model of Longuet-Higgins and Prazdny (1980). This model was designed to isolate the radial pattern of flow due exclusively to observer translation from the retinal flow resulting from both translation and eye rotation. It capitalizes on the fact that the image motion of two elements at different depths along the same visual direction will differ because of observer translation but not observer rotation. Taking the difference vectors along these depth discontinuities will cancel the contributions due to rotation, leaving only the contributions due to translation, thereby recovering the radial pattern of flow. In sparse environments, the visual system may be forced to rely on the motion of nonoverlapping elements in the same visual neighborhood. Rieger and Lawton's (1985) model was designed to cope with the noisy difference vectors that result from two nonoverlapping elements. The model is reasonably tolerant of noise (e.g., about 5° of heading error with 5% of noise).

Despite their differences, the preceding computational models share a common assumption, namely that the environment is populated exclusively by stationary objects. As a result, image motion is determined solely by a combination of the six parameters of observer movement. Any deviations are attributed to measurement error of the type described above. The world, however, is full of independently moving objects. When objects move independently of the observer, the resultant image motion is locally perturbed and hence is not purely a function of observer movement (Figure 1B). One approach to coping with moving objects is to treat perturbations in image motion due to moving objects in the same manner as perturbations due to measurement error. That is, the models described above that were designed to cope with perturbations induced by measurement error could be extended to handle perturbations induced by moving objects. However, the local deformation in optical flow induced by moving objects is categorically different from the perturbations of individual image vectors due to inadequate measurement. Thus, computational solutions to coping with intrinsic noise may be neither necessary nor sufficient to tolerate perturbations induced by moving objects.

Studies of Human Heading Perception in the Presence of Moving Objects

Recently, two studies concerned with human heading perception addressed the issue of moving objects (Royden & Hildreth, 1996; Warren & Saunders, 1995). These studies were similar in several respects: (a) Simulated observer movement was limited to linear translation; (b) the simulated environment consisted of frontoparallel random-dot plane or planes—a single plane for Warren and Saunders and two transparent planes for Royden and Hildreth; (c) displays included a single moving object depicted as a 2-D square made of random dots; and (d) both studies used the fixed camera angle technique (Cutting et al., 1992; Warren, Morris, & Kalish, 1988), thereby explicitly excluding rotational components from displays. In the fixed camera angle technique, gaze direction is deflected from heading direction by a fixed amount, whereas the FOE remains stationary but shifted away from the center of the screen. With simulated observer movement toward the frontoparallel plane (or planes), the FOE was located at the periphery of every display.

The findings of the two studies were similar as well; both reported accurate perception of heading in the presence of a moving object. Also common to both was a small but systematic pattern of bias in perceived heading direction when the moving object occluded the FOE. It is noteworthy that the direction of the observed bias differed in the two studies. Whereas Warren and

Saunders (1995) reported a bias in the direction of the object's FOE (opposite to the direction of object motion), Royden and Hildreth (1996) found a bias in the opposite direction, that is, in the direction of the moving object.

The Warren and Saunders (1995) study was an attempt to validate Hatsopoulos and Warren's (1990) template model in which the visual system pools over velocity vectors in the entire visual field, including noisy vectors generated by moving objects. Warren and Saunders extended the model to cope with moving objects by showing that a moving object, especially one in the central visual field, will result in greater activation of templates near the object's FOE. Thus, the presence of a moving object will bias perceived heading toward the object's FOE.

The Royden and Hildreth (1996) study was an attempt to validate Hildreth's (1992; see also Royden & Hildreth, 1999) motion parallax model, which was an extension of the algorithm (discussed above) introduced by Rieger and Lawton (1985). Whereas difference vectors taken from regions with stationary objects will point roughly toward the FOE (i.e., vectors consistent with respect to the FOE), those taken from regions with moving objects (i.e., vectors inconsistent with respect to the actual FOE) will point in arbitrary directions. Hence, the additional containment of the computations of optical flow due to a moving object can be accommodated by a consistency check that effectively filters out the noise in the image plane.

Despite their differences, a common property of both models is that robustness in the presence of moving objects is achieved by capitalizing on the redundancy in the flow field that occurs when the portion of the visual field corresponding to moving objects is relatively small compared with the portion of the visual field corresponding to the stationary environment. In Hildreth's (1992) model, the region of the visual field with the largest number of difference vectors that radiate outward from a location in that region is assumed to contain the heading direction. Assuming that moving objects do not take up a large portion of the visual field, the model is likely to select the region that contains the actual FOE. Once the region is selected, difference vectors that point to other regions can be removed from the computation and used to identify a moving object (or objects). The implication of this approach is that observer movement will be determined by the image motion of the largest region of consistently moving elements, regardless of whether the image motion in this region is actually due to observer or object motion.

The issue of how to distinguish between observer and object motion is circumvented in Warren and Saunders's (1995) model, because the model pools over vectors corresponding to both observer and object motion. This approach predicts that moving objects will always induce a bias of some sort, but assuming again that moving objects do not cover a large portion of the visual field, the relative contribution of vectors belonging to the rigid environment will effectively dampen the contribution of vectors belonging to the moving object. Consequently, the major factor determining the model's accuracy is the number of vectors corresponding to moving objects.

A consequence of both approaches is that vectors corresponding to the global motion of the observer, rather than the local motion of the object, are implicitly defined as those belonging to the portion of the visual field with the largest area of coherent motion (Hildreth, 1992) or the largest number of coherently moving elements (Warren & Saunders, 1995). Indeed, the experiments reported in both studies reflected this assumption, because only a single moving object was used, and because the ratio of the number of elements corresponding to the stationary environment to the number of elements corresponding to the moving object (i.e., the signal-to-noise ratio; SNR) was always considerably greater than 1. Yet, previous research suggests that self-motion is not distinguished from object motion on the basis of area of stimulation (Andersen & Braunstein, 1985; Warren & Kurtz, 1992) or the motion of the largest number of elements (Kim, Fajen, & Turvey, 2000; Kim & Turvey, 1998; van den Berg, 1992; Warren, Blackwell, Kurtz, Hatsopoulos, & Kalish, 1991). Thus, neither the area of stimulation nor the sheer number of elements should be used as the criterion by which moving objects are distinguished from the background environment.

A second assumption is that the observer moves rectilinearly. This assumption is critical, because the computational steps used to cope with moving objects in both models assume a unique, well-defined pattern corresponding to observer movement (viz., the radially expanding pattern associated with linear observer movement). Whereas such a well-defined pattern exists for linear translation, the global structure corresponding to curvilinear translation remains elusive. The optical flow resulting from observer movement along a circular path can be described in terms of a one-parameter family of concentric circles with a common center of rotation and the radius as the parameter. The corresponding retinal flow consists of image trajectories tracing hyperbolic paths (Figure 1C). However, the curvature of each hyperbola differs, complicating any attempt to provide a single encompassing description. Complicating matters further, the overall image pattern changes with a change in the parameter of the flow field (i.e., the radius of the observer's circular path). In summary, whereas a single pattern is associated with linear observer movement (i.e., radial expansion), an infinite number of patterns exist for curvilinear observer movement (i.e., a one-parameter family of hyperbolae), depending on the radius of the observer's path.

Because the Hildreth (1992) model works by taking difference vectors along depth discontinuities, the rotational component of flow due to curvilinear observer movement is eliminated in the same manner that the rotational component due to eye movements is eliminated in the model of Longuet-Higgins and Prazdny (1980; see above). Once the rotational component is removed, the resulting flow field is radial and contains an FOE corresponding to the observer's instantaneous direction of motion. Thus, by taking difference vectors, the Hildreth model is capable of restoring the single, well-defined pattern that is required to identify and segment the inconsistent vectors corresponding to the moving object. When one eliminates the rotational component due to curvilinear observer movement, however, information about the observer's curvilinear movement is also eliminated. Control of locomotion may require observers to perceive their future circular path, that is, the path the observer would follow by continuing to turn with constant path curvature (Kim & Turvey, 1998; Warren, Mestre, Blackwell, & Morris, 1991). Thus, once the visual system identifies and segments the elements corresponding to the moving object, it would have to restore the rotational component back to the flow field to compute the future path. Of course, the Hildreth model was designed to identify instantaneous heading, not the future path. Nonetheless, for this model to segment moving objects without

eliminating the information needed to judge the future path, it must proceed through a number of computationally demanding steps: (a) Compute difference vectors to eliminate rotational component, (b) identify the region with the largest number of difference vectors that radiate outward from a location in that region, (c) identify and segment inconsistent vectors corresponding to the moving object, (d) restore the rotational component that was removed in Step 1, and (e) estimate the future path.

With respect to Warren and Saunders's (1995) model, the main difficulty is that of template modeling in general, namely the number of templates required. To limit the number of templates in the context of eye rotations, Perrone and Stone (1994) added pursuit fixation and gaze-stabilization constraints. Additional templates would presumably be required to deal with curvilinear movement. Because of the absence of a unique, well-defined pattern of flow for curvilinear movement, the number of additional templates required would be unrealistically high. Furthermore, it is not clear how moving objects would influence such a system, especially when they trace curved paths. For linear movement, the perceived location of the FOE corresponds to a weighted average of the actual FOE and the FOE of the moving object. Given the absence of such a fixed local feature of the optical flow field in the more general context of curvilinear movement, a weighted averaging scheme does not seem possible.

In summary, both types of models incorporate steps to cope with moving objects that assume the existence of a single, well-defined pattern of optical flow. Whereas the Hildreth (1992) model is capable of successfully recovering such a pattern from the flow field produced by curvilinear observer movement, the visual system must eventually undo these operations to estimate the observer's curvilinear movement (i.e., the future path). In contrast, because the Warren and Saunders's (1995) model is incapable of recovering the well-defined pattern that it requires, it is unclear how this model could be generalized to account for curvilinear heading perception in the presence of moving objects.

Present Research

The experiments described here were carried out with the goal of determining an observer's capacity for perceiving direction of heading in the presence of moving objects, but in a more general context (i.e., locomotion along a curved path in the presence of multiple moving objects). The flow field simulated observer translation along a curved path that was either circular or elliptical. The extent to which the flow field was perturbed was controlled in terms of the object's path, the number of objects, and the object's transparency. First, the object either moved parallel to the observer or intersected the observer's path and either approached or retreated from the moving observer. Second, the number of objects introduced to the flow field varied from one to three. Third, the object was depicted as either transparent or opaque, or it was left black (i.e., drawn in the same color as the background). By measuring human observers' performance under these conditions, we hoped to further assess the perceptual capabilities of self-motion estimation in the presence of moving objects. Such manipulations also permitted us to evaluate existing models of heading perception, thereby complementing the research programs of computational vision scientists.

Whereas generalizations were sought with respect to some of the conditions examined, certain compromises were also made to simplify the task. The displays simulated observer movement along a curved path parallel to the ground. The simulated gaze direction was always fixed with respect to the instantaneous direction of heading. Furthermore, following the rationale behind Warren and Saunders's (1995) experiments—that is, (a) participants' perceptual performance would be best if eye movement was unrestricted, and (b) the visual system can discount the effects of eye rotation (cf. Royden, Crowell, & Banks, 1994; Warren & Hannon, 1990)—we let participants move their eyes freely during the experiment (but see Cutting, Vishton, & Braren, 1995, for the effect of a moving object on perceived direction of heading under pursuit fixation).

Four experiments were conducted. Experiment 1 examined perceived heading from a flow field simulating observer translation along a circular path. A single object was introduced to the flow field that moved parallel to or intersected the observer's path. Experiments 2–4 examined the effect of multiple moving objects on perceived heading. The observer's path also varied from circular to elliptical. In Experiments 1 and 2, objects were depicted as transparent; that is, objects' surfaces were invisible. In Experiments 3 and 4, the surface properties of objects were specifically manipulated to examine the effect of dynamic occlusion; that is, objects were depicted either as transparent, opaque, or black. In Experiments 1–3, the object receded away from the observer into the distance. The direction of object motion was reversed in Experiment 4 so that the object approached the observer.

Experiment 1: One Moving Object

Experiment 1 was conducted as a preliminary study to see whether human observers were indeed capable of perceiving heading direction while negotiating a curved path in the presence of moving objects. To minimize the complexity of the optical pattern involved, we simplified the display in the following ways. First, displays simulated observer movement along a circular path parallel to a ground plane. Second, only a single object, which glided over the ground plane, was introduced to the flow field. Nonetheless, the resultant flow pattern was complicated, because the parameters defining the flow field varied as a part of experimental control. For example, the radius of the observer's path varied, producing varying patterns of image motion corresponding to the background surface or the global structure of the flow field. The path of the object also varied in four different ways (see Figure 2). In Object Paths A and B, the moving object followed a path parallel to but inside or outside the observer's path, respectively. In Object Paths C and D, the moving object intersected the observer's path from outside to inside or inside to outside, respectively. All objects appeared from behind the observer, passed by, and eventually retreated into the distance.

Method

Participants. A total of 12 participants took part in the experiment. There were 10 who were undergraduate students who participated in partial fulfillment of a course requirement, and 2 were graduate students at the University of Connecticut who participated voluntarily. All participants had normal or corrected-to-normal vision.

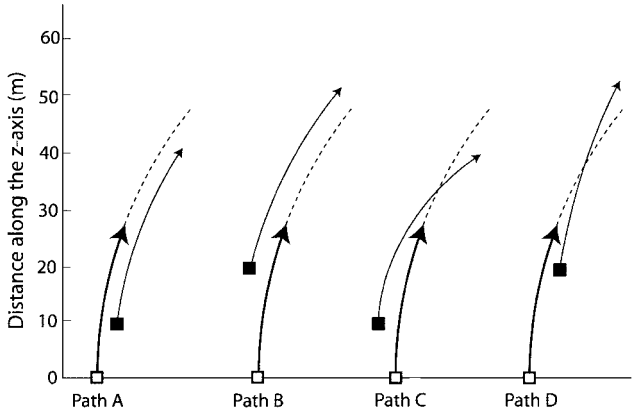

Figure 2. Plan view of the four object paths used in Experiment 1 for the $R = 80$ m condition. Initial positions for the observer and the object are indicated by white and black squares, respectively. Final positions for the observer and the object are indicated by arrowheads. Object paths are depicted by thin lines, and observer paths are depicted by thick lines. The projections of the observer paths are indicated by dotted lines.

Apparatus. Displays were generated by a Silicon Graphics Indigo2 R4400 workstation and presented on a 19-in. (48.3-cm) screen refreshed at 60 frames/s. The display had a pixel resolution of 1280 (horizontal) × 1080 (vertical) pixels and subtended 42° (horizontal) × 32° (vertical). Participants sat 50 cm in front of the display screen, a distance that coincided with the simulated viewing distance, and viewed displays from a chin rest. Each display lasted about 2 s (120 frames).

Stimuli. Displays simulated observer movement parallel to a random-dot ground plane along a circular path. The ground plane consisted of 150 dots placed randomly within each cell of an appropriately scaled grid (for a detailed description of these manipulations, see Kim & Turvey, 1998). The dots were single white pixels drawn on a black background. As a dot passed by the observer and out of view, a new dot was introduced in the far end of this region, thereby maintaining approximately the same number of dots during the duration of each trial.

The observer's simulated tangential speed was held constant at 13.2 m/s (or 30 mph). Accordingly, angular velocity, $\omega = v/R$, varied as a function of R (radius of the observer's path). Hence, in the $R = 80$ m condition, each surface element rotated at 9.5 degrees/s (0.165 radians/s).

The moving object appeared as 80 white dots randomly positioned in a 3-D cube (more precisely, a hexahedron; i.e., a polyhedron of six faces), roughly the size of a minivan with dimensions of 1.8 m (width; W) × 1.6 m (height; H) × 4.7 m (depth; D), and glided over the ground surface. The object moved at an angular velocity of 3 degrees/s (0.05 radians/s) faster than the observer. Note that the radius of the object's motion trajectory varied as an independent variable. Hence, the corresponding tangential speed varied. The direction of optical motion of the object was opposite to that of the surface elements. That is, all surface elements moved from far to near, eventually receding behind the observer. The object, on the other hand, moved from near to far.

The moving object followed one of the four paths shown in Figure 2. In Object Paths A and B, the object moved parallel to the observer with the same center of rotation as the observer's trajectory but inside the observer's path in A and outside the observer's path in B. In Object Path A, the radius of the object's trajectory was 4 m larger than the radius of the observer's trajectory, whereas, in Object Path B, it was 3 m less than the radius of the observer's trajectory. In Object Paths C and D, the object started to move toward the observer's path and eventually crossed it during the display, either by shrinking its radius in Object Path C or by increasing its radius in Object Path D by 0.06 m per frame (7.2 m for the duration of trial). At the start of the display, the object lay 10 m in front of the observer along the z-axis in Object Paths A and C; whereas the object appeared 20 m in front of the observer in Object Paths B and D. In some conditions, the object was initially within the field of view and receded into the distance. In other conditions, it was necessary for the object to be initially outside the field of view. In such conditions, however, the object immediately appeared on the screen and receded into the distance.

Design. Heading accuracy was assessed in terms of heading angle, the same measure used by Warren, Mestre, et al. (1991). Heading angle was the visual angle defined by a target on the ground, the point of observation, and the point at which the observer's path passed the target (see Warren, Mestre, et al. for further details; see also Kim & Turvey, 1998). Heading angle varied randomly among values of ±0.5°, ±1°, ±2°, and ±4°. Positive values of heading angles indicated that the observer's path lay inside of the target, and negative values indicated that the observer's path lay outside of the target.

The radius of the observer's path (R) also varied randomly among ±80 m, ±120 m, ±160 m, and ±320 m values. Positive values correspond to a right-hand turn, and negative values correspond to a left-hand turn.

These manipulations yielded a 4 (object path) × 4 (R) × 2 (turn direction) × 4 (heading angle) × 2 (target location) repeated measures design with 256 trials. All variables were controlled within subjects.

Procedure. Participants were instructed that the displays would depict the appearance of the ground when one travels along a curvilinear (turning or winding) path or road. Participants were also told that they would see groups of dots that moved together, depicting a moving object such as a car. Participants were told to try not to let the moving object influence their judgments. Participants initiated the displays by pressing the space bar on the computer keyboard. Participants watched the display until it stopped and a blue vertical bar appeared on the ground surface. At that time, participants pressed one key if the path of travel seemed to be to the left of the vertical bar and another key if the path of travel seemed to be to the right of the vertical bar.

Prior to the main experiment, a short practice session was provided to allow participants to become familiar with the experimental setup. The practice session comprised eight trials constructed by crossing four radii (±240 m and ±480 m) with two heading angles (±5°). The object followed Object Path A. Feedback was provided during the practice session but was not given during the experiment.

Data analysis. Following Warren, Mestre, et al. (1991; see also Kim & Turvey, 1998), heading accuracy was evaluated in terms of heading thresholds. Heading threshold was determined by fitting the data at each condition with an ogive, which we then regressed on heading angle. We adopted as the threshold the angle at which the regression line reached 75% correct. The first phase of this conversion, that is, fitting the data with an ogive, was accomplished by performing a z transformation on the percentage of correct responses at each heading angle, assuming that heading detection would be easier with increase in heading angle. When each participant's data for each Object Path × R condition were collapsed over the signs of R and heading angle to calculate the percentages of correct responses, there were only four observations at each heading angle, too few data points to show a trend. To perform the analysis, we increased the sample size by further collapsing the data over object path or R. Because of this, we describe two separate measures of threshold: threshold at each condition of R and threshold at each condition of object path. One participant performed below threshold at all heading angles in the $R = 80$ m condition. Consequently, data for this participant were excluded from that condition. Heading bias was measured as the percentage of outside responses, following Warren, Mestre, et al. (1991). A 50% outside response rate indicates no bias.

Results and Discussion

The percentages of correct responses for the four object paths as a function of R are presented in Figure 3A. Overall accuracy was

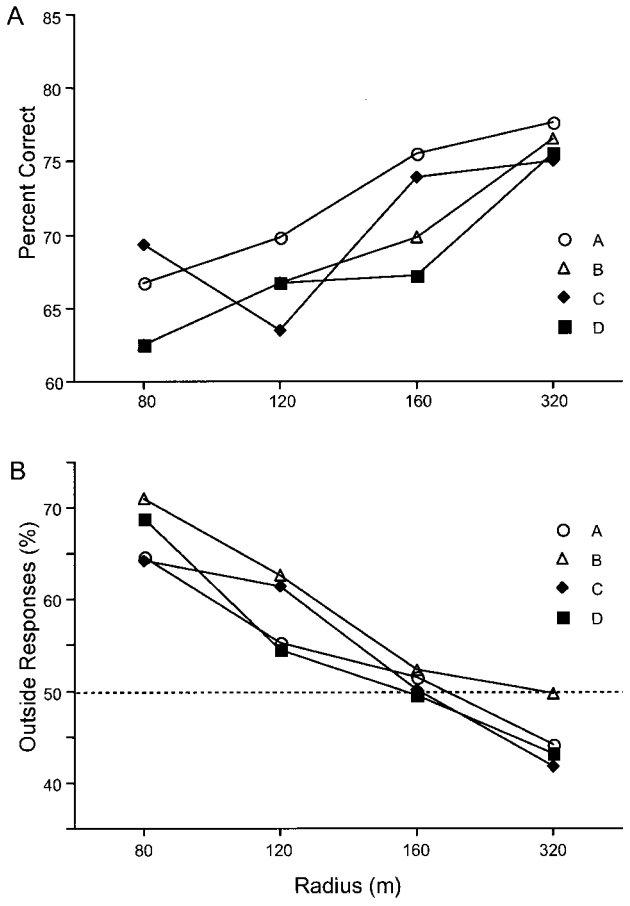

Figure 3. Percentages of correct responses (A) and percentages of outside responses (B) in Experiment 1 for the four object paths as a function of the radius of the observer's path. The horizontal reference line at 50% (in B) indicates where an equal number of inside and outside responses would be made, suggesting no bias.

70%, a level comparable to that observed in a similar condition but without a moving object (e.g., 73% in Experiment 1 of Kim and Turvey, 1998, in which circular heading was examined with the same *R* parameters). Results were collapsed over sign of curvature and sign of heading angle. A 4 (object path) × 4 (*R*) × 4 (heading angle) analysis of variance (ANOVA) revealed significant main effects of *R*, $F(3, 33) = 7.79$, $p < .01$; and heading angle, $F(3, 33) = 111.68$, $p < .01$. No other main effects or interactions were significant. The effect of *R* was consistent with prior findings (Kim & Turvey, 1998; Warren, Mestre, et al., 1991) in which circular heading was shown to be more difficult to determine for smaller *R* and, therefore, for larger curvature of the movement trajectory.

Mean thresholds are shown as a function of *R* in Figure 4A and as a function of object path in Figure 4B. An ANOVA for *R* using thresholds as a dependent measure showed a significant effect of *R*, $F(3, 30) = 8.07$, $p < .01$, replicating the first ANOVA. In another ANOVA for object path on thresholds, the effect of object path was not significant, $F(3, 33) = 2.40$, $p > .05$, also replicating the first ANOVA. The mean threshold of 2.2° was slightly higher than the overall thresholds of 1.4° for circular heading reported in Warren, Mestre, et al. (1991) and 1.7° reported in Kim and Turvey (1998) but nonetheless accurate enough to support successful navigation through the environments. Note that Cutting (1986) estimated that a heading accuracy of 4.2° is needed for drivers to maintain a speed of 13.2 m/s to brake properly for a pedestrian or animal. In general, accuracies in the range of 1°–3° are assumed necessary for obstacle avoidance at speeds covering walking, running, and driving (Cutting et al., 1992).

The percentage of outside responses, our measure of heading bias, for each object path is presented as a function of *R* in Figure 3B. To further evaluate response bias, we compared the percentages of outside responses with 50%, which indicates no bias. First, the overall outside bias of 55% was not significantly different from 50%, $t(11) = 1.10$, $p > .05$. For each condition of object paths of A, B, C, and D, the responses were 54%, 59%, 54%, and 54%, respectively. None of these reached statistical significance. For each condition of observer's paths of $R = 80$, 120, 160, and 320, the responses were 67%, 59%, 51%, and 45%, respectively. Of these, only $R = 80$ m, $t(11) = -2.87$, $p < .05$, showed an outside bias. The latter effect in conjunction with the *R* effect revealed by the first ANOVA on accuracy was consistent with prior findings (Kim et al., 2000; Kim & Turvey, 1998; Warren, Mestre, et al.,

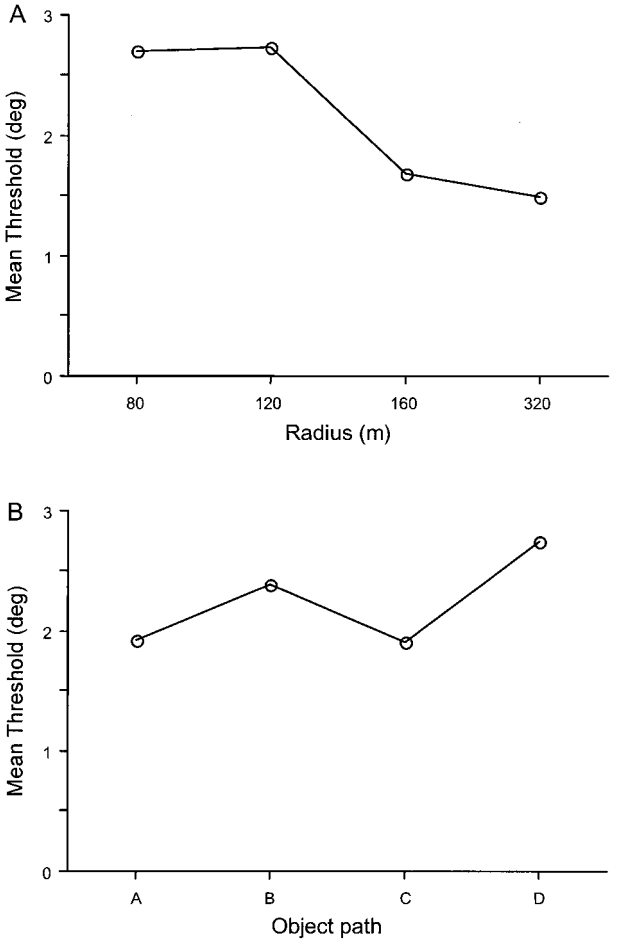

Figure 4. Mean heading threshold in Experiment 1 as a function of the radius of the observer's path (A) and as a function of the object path (B). deg = degrees.

1991) in which the degree of bias was shown to be a function of path curvature or an inverse function of *R*—the larger the curvature, or the smaller the radius, of the observer's path, the bigger the bias, with the direction of bias predominantly outside the observer's path.

The lack of bias observed in Experiment 1 contrasts with the response patterns observed in Royden and Hildreth (1996) and Warren and Saunders (1995; but see Cutting et al., 1995, for a similar result). For Warren and Saunders (1995), in particular, bias was considered crucial as a way to evaluate various computational models. In their study, however, bias was observed only when the object obscured the FOE. Warren and Saunders attempted to address this finding by weighting vectors near the FOE more heavily in the computation. Recall that for linear translation along the depth axis, a well-defined radial pattern arises with the FOE corresponding to the direction of translation. As a result, when vectors associated with different motion types (i.e., observer and object) are pooled as a weighted sum, another FOE can be obtained. That FOE, which deviates from the actual FOE corresponding to the observer's direction of heading and its location, will be a direct function of the ratio of the corresponding image vectors. In contrast, when translation occurs along a curved path, the resultant flow field lacks a singularity and, more important, a single encompassing description. Accordingly, it is not clear how a weighted averaging scheme can be effective to handle the disturbance in the flow field by the moving object in the more general context of curvilinear movement nor can it explain a pattern of bias under such a condition.

Taken together, participants in this experiment were quite reliable in perceiving circular heading, even in the presence of a moving object. The overall mean threshold of 2.2° was well below the required accuracy of 4.2° necessary for a proper braking at the simulated speed. The observed bias pattern reveals little indication of the influence of the moving object. In short, it is not clear that participants' perception of circular direction of heading was influenced by the presence of moving objects.

It can be argued, however, that the values of thresholds observed in this study may be comparable, but not equal, to those reported in similar conditions without moving objects (e.g., Kim & Turvey, 1998). In fact, the larger values may suggest poorer performance. Is the difference in threshold values systematic to the extent that it can be attributed to the presence of the moving object? Experiment 1 of Kim and Turvey (1998) used the identical manipulations of heading angle and observer's path and the identical number of participants (12 participants in both studies) and therefore provided a way to check this possibility. Although that study examined the effect on perceived circular heading of two different types of noise (i.e., random vs. vertically displaced noise), the resultant levels of SNR (2.0 or 4.0) were shown to be too high to have any effect on perceived heading (see Kim et al., 2000). Therefore, the presence of noise can be safely ignored. Thus, for the sake of comparison, the percentages of correct responses in that study were combined across noise types and was compared with the percentages of correct responses of the present study. According to this analysis, the presence (or absence) of a moving object in the simulated flow field was not a reliable effect, $F(1, 22) = 2.01$, $p > .05$; there were no interactions involving this effect. The results of this additional analysis corroborates our suspicion that the effect of moving objects on perceived heading was indeed minimal, at least within the limits of Experiment 1.

In fact, the results of Experiment 1 may be more consistent with the findings from research (Kim & Turvey, 1998; van den Berg, 1992; Warren, Blackwell, et al., 1991), showing that heading perception is robust against noise, degrading smoothly as the amount of noise increases. van den Berg (1992), in particular, demonstrated that heading judgments degrade gradually with some indication of heading awareness, even at an SNR level as low as 0.5. Perhaps, the presence of moving objects under such circumstances may be more noticeable. In Experiment 2, we explored this possibility.

Experiment 2: Multiple Moving Objects

Experiment 2 examined the effect of many moving objects on perceived heading. To this end, we introduced three objects to the flow field. Recall that the two studies conducted by Royden and Hildreth (1996) and Warren and Saunders (1995) introduced only a single moving object. Moreover, the density of the image vectors corresponding to object motion was held extremely low in comparison to the density of image vectors corresponding to the background, thereby circumventing the issue of how the visual system distinguishes those two different types of image vectors. In terms of SNR (ratio of number of elements on the object to number of elements in stationary environment), for example, the levels used in both studies were 6.3 in the Royden and Hildreth study and 12.0 and 5.5 in the Warren and Saunders study, both of which were too high to have any measurable effect on perception (e.g., Kim et al., 2000; Kim & Turvey, 1998). We specifically held the combined dot density of the moving objects above that of the background by depicting each object by 80 random dots (for a total of 240) and the background environment by 150 dots. This resulted in more noisy, or inconsistent, vectors in the flow field than signal, or consistent, vectors. The resultant SNR was 0.63, a level previously shown to degrade perceived heading judgments for noise elements that were randomly distributed and moving in random directions (Kim & Turvey, 1998; van den Berg, 1992). For reference, the level used in Experiment 1 was 1.88 (80 dots for a moving object vs. 150 dots for the environment).

As in Experiment 1, object paths varied as well. Two of the three objects always moved along paths parallel to the observer's path, one inside and one outside, whereas the other moved along one of the four paths used in Experiment 1 (see Figure 5). This manipulation was to gain a deeper understanding of the overall effect of moving objects on perceived heading.

We also increased the variety of the simulated observer's path to include elliptical as well as circular paths (see Kim & Turvey, 1998, for perceived heading on circular and elliptical paths but without moving objects). During circular motion, the curvature of the observer's path remains constant and the flow field is steady. That is, the velocity vector corresponding to each point on the optic array remains constant in both direction and magnitude. During elliptical motion, path curvature changes, and the flow field is unsteady. Consequently, velocity vectors at points on the optic array change. Whereas for linear and circular motion the optical flow corresponding to the background against which object motion takes place is at least constant, for elliptical motion, the optical flow corresponding to the background is changing.

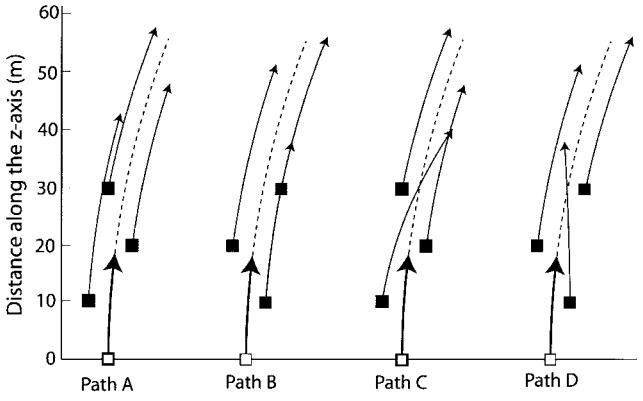

Figure 5. Plan view of the four object paths used in Experiment 2 for the $R = 160$ m condition. Initial positions for the observer and the objects are indicated by white and black squares, respectively. Final positions for the observer and the objects are indicated by arrowheads. Object paths are depicted by thin lines, and observer paths are depicted by thick lines. The projections of the observer paths are indicated by dotted lines.

Method

Participants. A total of 8 graduate students at the University of Connecticut participated voluntarily. All participants had normal or corrected-to-normal vision.

Stimuli. As in Experiment 1, displays simulated observer movements parallel to the ground plane and lasted 2 s (120 frames). Unlike Experiment 1, in Experiment 2 the simulated curvilinear paths of observer movement followed elliptical as well as circular trajectories. The curvilinear path was controlled as a ratio between two semiaxes in which *a* lies along the *x*-axis (along the observer's frontal plane) and *b* lies along the *z*-axis (along the tangential heading direction). Aspect ratios varied randomly among ±160:160 m, ±320:320 m, ±160:320 m, and ±320:160 m (positive values correspond to a right-hand turn and negative values correspond to a left-hand turn). The first two ratios corresponded to circular paths, and the last two corresponded to elliptical paths. The two elliptical paths were further distinguished in terms of their axes of elongation. In the 160:320 path, the *z*-axis is the axis of elongation; in the 320:160 path, the *x*-axis is the axis of elongation.

Flow velocity was controlled as angular velocity, which was held constant at 3 degrees/s or 0.05 radians/s. Consequently, tangential velocity $v = R\omega$ varied, depending on the curvature of the flow line on which a given surface element traveled. Hence, for the two circular paths, the corresponding tangential velocities were 8 m/s (18 mph) for the 160 m *R* condition and 16 m/s (36 mph) for the 320 m *R* condition. For the two elliptical paths, the velocity of a surface element varied depending on its location along the path. For example, the element's tangential velocity is greatest when it passes the tip of the major axis of the path and least when it passes the tip of the minor axis.

Of the three objects added to the flow field, two moved parallel to the observer's path, one inside and the other outside. The objects had slightly different physical dimensions. The first two objects were roughly the size of a minivan with dimensions of 1.8 m (W) × 1.6 m (H) × 4.7 m (D) and 1.9 m (W) × 1.9 m (H) × 4.7 m (D), respectively. The third object was the size of a sports car with dimensions of 1.6 m (W) × 1.5 m (H) × 4.1 m (D). Each object was made of 80 white dots randomly positioned within its contour. The first object moved at an angular velocity of 0.05° per frame or 0.05 radians/s, relative to the observer, whereas the latter two objects moved at the same angular velocity of 0.04° per frame or 0.04 radians/s, relative to the observer.

The geometry of the four object paths with respect to the observer's path is depicted in Figure 5. Across the four object path conditions, there was always one object outside and one object inside the observer's path at the beginning of each trial. In Object Paths A and C, the third object was initially outside the observer's path; whereas, in Object Paths B and D, it was initially inside the path. All objects moved along a curved trajectory with the same center of rotation as the observer's trajectory. In terms of aspect ratio used to define an observer's path denoted as *x*:*z*, the first object's path can be denoted as $(x + 4)$:$(z + 4)$, the second as $(x - 3)$:$(z - 3)$, and the third as $(x \pm 3)$:$(z \pm 3)$, depending on its location (positive value corresponds to outside and negative value corresponds to inside of the observer's path). When the third object followed a $(x - 3)$:$(z - 3)$ path, the second and third objects were on identical paths but differed in depth. The three objects were initially 10, 20, and 30 m in front of the observer along the *z*-axis. In Object Paths A and B, all objects moved parallel to the observer and maintained the same trajectory as the observer. In Object Paths C and D, the object closest to the observer started to move toward the observer's path and eventually crossed it during the display. In Object Path C, the object outside the observer's path was made to cross the observer's path by shrinking its aspect ratio by 0.06 m per frame (7.2 m for the duration of the trial). In Object Path D, the object inside the observer's path was made to cross the observer's path by increasing its aspect ratio by 0.05 m per frame (6.0 m for the duration of the trial). Because of the variations in observer and object paths, the projected image size of each object varied during a trial, as shown in Table 1.

Design. Three variables were controlled within subjects: object path, curvature of the observer's path, and heading angle. The curvature of the observer's path varied among ±160:320, ±320:160, ±160:160, and ±320:320 m. Heading angle was defined as in Experiment 1 and varied randomly among four values: ±0.5°, ±1°, ±2°, and ±4°. This yielded a 4 (object path) × 4 (curvature) × 2 (turn direction) × 4 (heading angle) × 2 (target location) repeated measures design with 256 trials.

Procedure. As in Experiment 1, a short practice session preceded the main experiment. The eight practice trials incorporated four circular paths ($R = \pm 240$ m or ±480 m) with two heading angles (±5°). The practice

Table 1
Maximum and Minimum Image Sizes of Each Moving Object by Curvature of Observer's Path in Experiment 2

Observer's path (m)	Object A		Object B		Object C	
	Max. (deg)	Min. (deg)	Max. (deg)	Min. (deg)	Max. (deg)	Min. (deg)
160:320	4 × 2	2 × 1	7 × 5	2 × 2	2 × 2	1 × 1
320:160	14 × 10	6 × 4	6 × 6	4 × 5	8 × 6	4 × 3
160:160	15 × 9	5 × 4	6 × 5	3 × 3	4 × 3	3 × 2
320:320	7 × 5	3 × 2	11 × 9	4 × 3	3 × 3	2 × 2

Note. Max. = maximum; Min. = minimum; deg = degrees.

trials contained two moving objects, one inside and one outside of the observer's path, that followed Object Path A. Feedback was provided during the practice session but was not given during the experiment.

Results and Discussion

The percentages of correct responses for the four object paths are presented as a function of curvature of the observer's path in Figure 6A. Overall accuracy was 69%, comparable to that observed in Experiment 1. For further analysis, we collapsed the results over sign of curvature and sign of heading angle and entered into a 4 (object motion) × 4 (curvature) × 4 (heading angle) ANOVA. Only the main effects of heading angle, $F(3, 21) = 62.02$, $p < .01$, and curvature, $F(3, 21) = 4.21$, $p < .05$, were significant. With respect to the effect of curvature, performance in the 160:320 m condition ($M = 74\%$) was significantly different from performance in the 320:160 m ($M = 64\%$), 160:160 m ($M = 68\%$), and 320:320 m ($M = 72\%$) conditions. Performance in the latter three conditions was not significantly different.

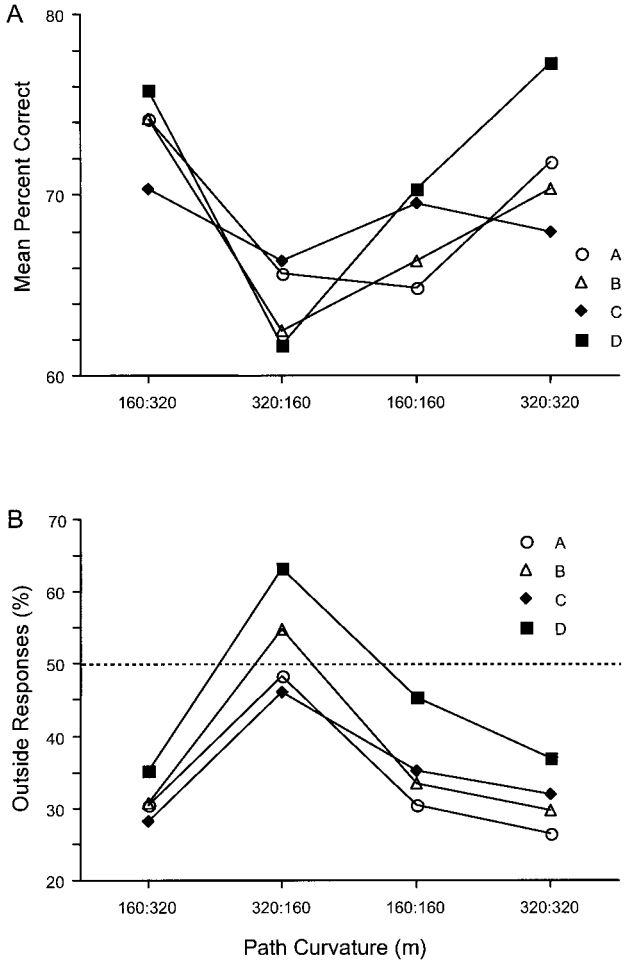

Figure 6. Percentages of correct responses (A) and percentages of outside responses (B) in Experiment 2 for the four object paths as a function of the curvature of the observer's path. The horizontal reference line at 50% (in B) indicates where an equal number of inside and outside responses would be made, suggesting no bias.

Mean heading thresholds are shown as a function of curvature of the observer's path in Figure 7A and as a function of object path in Figure 7B. The overall mean heading threshold was 2.4°, comparable to the value observed in Experiment 1, and also within the range required for steering locomotion accurately at the simulated speed. Two separate ANOVAs revealed no main effects of curvature, $F(3, 21) = 2.54$, $p > .05$; and object path, $F(7, 31) = 1.07$, $p > .05$.

The percentages of outside responses for the four object paths are presented as a function of the curvature of the observer's path in Figure 6B. With the mean overall outside bias of 40%, participants in this experiment, unlike those in Experiment 1, appeared to have preferred the inside of the observer's future path, but that tendency was not significantly different from 50%, $t(7) = -1.72$, $p > .05$. In terms of object paths, similar tendencies were observed (34% in A; 37% in B; 35% in C; 45% in D), but none reached statistical significance. In terms of curvature of the observer's path, apparent inside tendencies were observed in the 160:320 m ($M = 31\%$), 160:160 m ($M = 36\%$), and 320:320 m ($M = 31\%$) conditions; whereas the response pattern tended to be outside in the 320:160 m condition ($M = 53\%$). However, these tendencies were statistically significant only in the 160:320 and 320:320 conditions, $t(7) = -4.27$, $p < .01$, and $t(7) = -3.00$, $p < .05$, respectively. Note that these two conditions are those in which curvatures of the observer's paths are smallest. It is interesting that these are the same conditions that induced inside biases in Kim and Turvey's (1998; see their Experiments 2 and 3) study, albeit their study examined perceived heading along curvilinear paths without any moving objects. Taken together, the bias pattern observed in Experiment 2 largely replicates prior findings in similar conditions, minimizing the role played by moving objects on perceived curvilinear heading.

The key issue examined in Experiment 2 was the extent to which human observers could detect the consequences of their movements when the majority of image vectors in the flow field were not induced directly by their movements but by moving objects. The results indicate that judgments were quite accurate, on par with judgments in Experiment 1 in the presence of a single moving object. How would an increase in the number of image vectors corresponding to moving objects influence the models proposed by Hildreth (1992) and Warren and Saunders (1995)?

Because Hildreth's (1992) model uses average velocity vectors within small regions to compute velocity differences, increases in the number of elements corresponding to moving objects per se would not influence heading estimates. Rather, the real requirement of the Hildreth model is that moving objects do not occupy a larger area of the visual field than the stationary background. Because this requirement was fulfilled for the entire display duration, one would expect performance to be unaffected. Thus, accurate performance in the present experiment is consistent with the Hildreth model.

In contrast, recall that in Warren and Saunders's (1995) model, heading estimation was performed by pooling all the image vectors (including noisy vectors) over the entire flow field, weighting vectors in the center of the visual field more heavily. For this model to reliably estimate heading, there must be considerably more vectors corresponding to the stationary background than to the moving object (or objects); hence, local perturbations in the flow field induced by moving objects can easily be dampened out

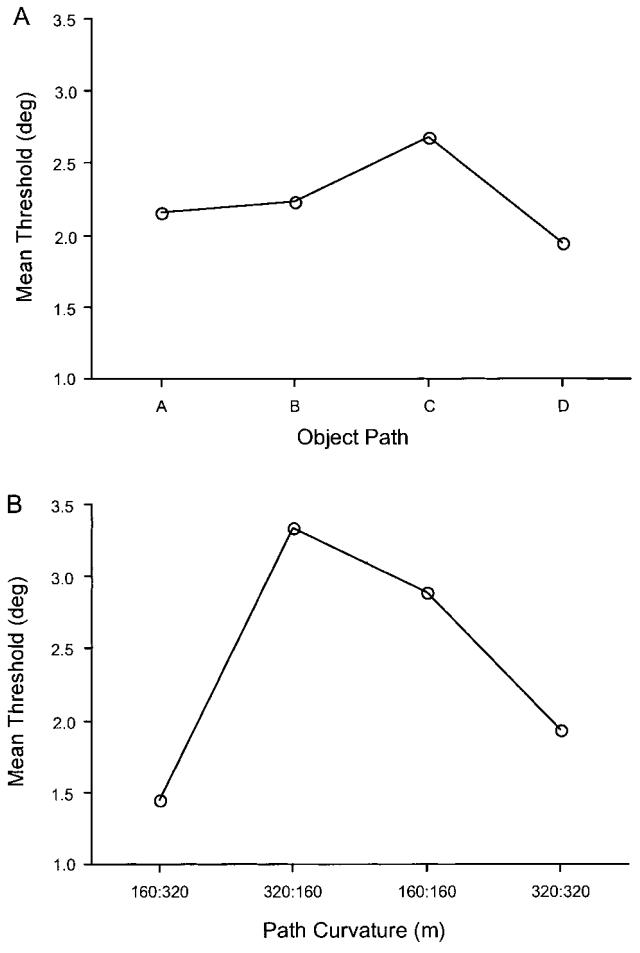

Figure 7. Mean heading threshold in Experiment 2 as a function of the object path (A) and as a function of the curvature of the observer's path (B). deg = degrees.

by the majority of the vectors corresponding to the moving object. As the number of vectors corresponding to moving objects increases, however, performance should decrease. Thus, the fact that heading accuracy with three moving objects was commensurate with one moving object is inconsistent with the Warren and Saunders (1995) model. Furthermore, because their model weighs image vectors in the center of the visual field more heavily, one would expect additional biases when moving objects intersect the observer's path. However, there were no significant effects of object path on measures of accuracy or bias.

In general, the results bring into question the assertion that the visual system is robust against noise with performance degrading gradually with increased noise density (e.g., van den Berg, 1992; Warren, Blackwell, et al., 1991). Whereas reliable performance, despite multiple moving objects dominating the visual field, corroborates this observation, consistent performance (i.e., no degradation), despite two additional objects in the flow field or decreased SNR (1.88 in Experiment 1 vs. 0.63 in Experiment 2), contradicts it. Instead, the results are more consistent with the conclusions of Kim et al. (2000). Of particular relevance to the present study is Kim et al.'s (2000) Experiments 1 and 2 in which nonrigidity of the environment was examined through the manipulation of two types of noise. In their *ground* condition, noise was introduced to the ground plane, perturbing the global pattern of the flow field, whereas, in their *medium* condition, noise was introduced to the flow field like snow flakes. They observed two contrasting patterns. In the ground condition, performance degraded gradually as a function of SNR, finally reaching asymptote at SNR = 0.5; these results are consistent with those of van den Berg (1992). In the medium condition, however, performance remained intact even at an SNR level as low as 0.08 (40 signal dots against 480 noise dots). On the basis of these results, Kim et al. concluded that it is not the noise or its density per se that matters but whether the noise affects the global pattern of the flow field that constrains heading perception. That is, when the flow pattern remains intact despite the presence of noise, accurate perception occurs; when the flow pattern is impaired, perception degrades likewise. It must be the case then that, despite apparent perturbation of the flow field induced by multiple moving objects, the underlying global pattern of the flow field remains intact, providing the information for direction of curvilinear heading. We return to this issue in the General Discussion.

In summary, despite the increased perturbation arising from two additional objects in the flow field, performance in Experiment 2 remained comparable to that observed in Experiment 1. The question still remains as to what constitutes the requisite information for direction of curvilinear heading in such a perturbed flow field. To further pursue this question, we manipulated, following Warren and Saunders (1995), the surface properties of the object in Experiments 3 and 4.

Experiment 3: Transparency of the Objects

In Experiments 1 and 2, the objects were depicted as transparent. Hence, all texture elements constituting the background surface, including those covered by the object, were projected to the point of observation. In contrast, the environment in which people live is typically occupied by opaque objects. Because light reflected from the surfaces of objects travels in a straight line, opaque objects block some background elements from being projected to the point of observation. Thus, there is no projective correspondence between the background texture elements and the corresponding optical elements for unprojected hidden surfaces.

A further challenge arises when the observer and the object are both in motion, the situation that is the focus of the present study. The perturbation induced by an opaque object moving in the field of view is categorically different from the pattern of perturbation induced by a transparent object. How can observers register the requisite information for determining their direction of locomotion despite the hidden surfaces occluded by a moving object?

In an attempt to examine the contrasting optical effects induced by moving objects, Warren and Saunders (1995) created objects with three different surface properties: transparent, opaque, and black. Transparent objects were created as described in the two preceding experiments (Figure 8A). For opaque objects, a black silhouette of the object was drawn first, and then the object's texture elements were added to the silhouette (Figure 8B). Black objects were depicted as textureless black silhouettes (Figure 8C).

These manipulations yielded two distinct optical effects that could be used to evaluate different computational algorithms. First,

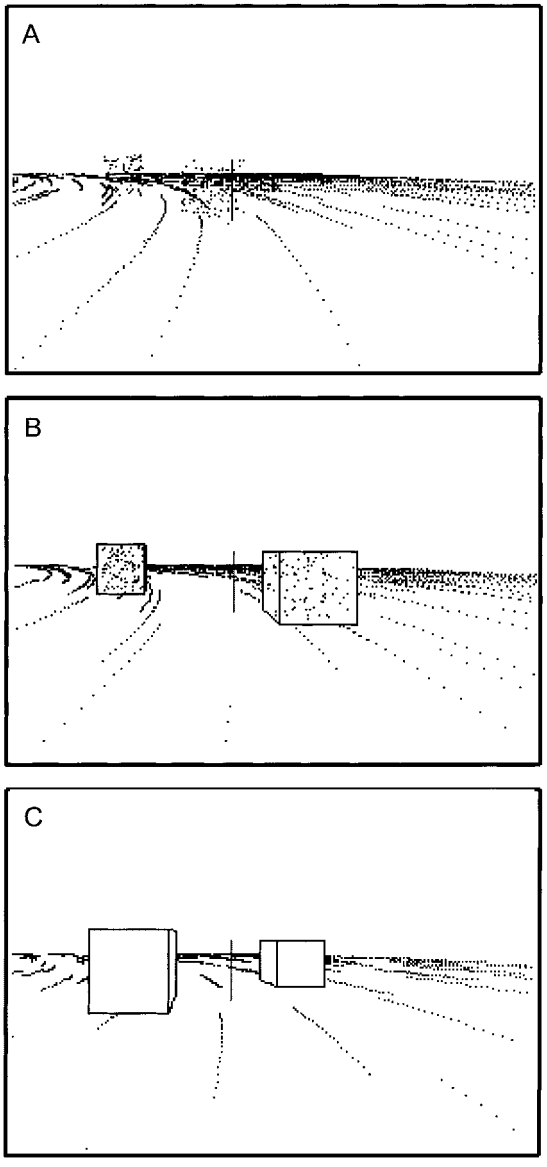

Figure 8. Displays used in the transparent (A), opaque (B), and black (C) object conditions in Experiments 3 and 4. The figure simulates an observer's movement along a circular path with a radius of 160 m and direction of turn toward the left. The vertical bar identifies the observer's heading. Optical flow lines of individual surface elements were produced by overlaying 60 frames, whereas the regions corresponding to moving objects from a single frame were shown with additional contours in B and C to enhance the visibility of the objects. In the actual experiment, displays were presented one frame at a time such that the flow lines were not apparent, and the objects (in B and C) in the displays were black, as was the background.

when both the observer and the object are in motion, tracing linear paths of their own, observer and object movement can be disambiguated by their distinct foci of expansion. Hence, models such as Hildreth's (1992) motion parallax model can use the relative motion between those image vectors corresponding to the object and those corresponding to the background as the optical basis for segmenting the moving object from the self-motion component. In addition, because opaque and black objects produce little to no relative motion, transparent objects can be expected to induce more accurate heading judgments than opaque or black objects.

Second, manipulating surface properties also has differential effects on SNR. SNR is highest in the black condition, followed by the transparent conditions and opaque conditions, in that order. Consequently, in Warren and Saunders's (1995) template model—which hypothesizes that the visual system simply pools over the entire velocity vector field without first segmenting the object—image vectors associated with objects (i.e., noise) will distort image vectors specifying the observer's heading direction (i.e., signal). Thus, the model predicts that the observer's judgments should be biased in the presence of transparent and opaque objects but not in the presence of black objects. The model also predicts poorer performance with opaque than transparent objects.

Warren and Saunders (1995) found that performance was poorest with an opaque object, somewhat degraded by a transparent object (especially when the object crossed the FOE), and virtually unchanged with a black object. The results were interpreted as support for a template model that detects global flow patterns by pooling over the entire velocity vector field, albeit weighting more heavily those vectors in the center of the field. Whereas Warren and Saunders observed the largest heading bias in the opaque condition with the mean bias in the order of 3.7°, Royden and Hildreth (1996) observed a rather small bias ($M \leq 0.9°$) across the conditions they examined when using an opaque object. It is interesting, however, that both studies found the highest heading accuracy—with virtually no bias—in the black object condition.

As underscored in the introduction, only when the observer and the object both move along linear paths of their own can the resultant flow field be described in terms of a single, well-defined pattern of flow (i.e., radial) with a fixed feature of optical flow (i.e., the FOE). Both Hildreth's (1992) and Warren and Saunders's (1995) model depend on this well-defined pattern to cope with moving objects. Although the Hildreth model is capable of recovering this pattern from the flow field induced by curvilinear observer movement, the same operation that recovers this pattern removes the rotational component of flow that is required to estimate the observer's curvilinear movement.

There is, however, another optical pattern associated with moving objects that is not used by either model but arises regardless of whether the observer's path of locomotion is linear or curvilinear. This pattern, referred to as *dynamic occlusion*, is characterized by a progressive deletion of the background texture at the leading edge of the object and progressive accretion at the trailing edge of the object (Gibson, 1968, 1979/1986; Gibson, Kaplan, Reynolds, & Wheeler, 1969; Kaplan, 1969). If the visual system can exploit dynamic occlusion as an additional source of information for segmentation, heading judgments should be better, or at least no worse, with opaque and black objects than with transparent objects.

To further evaluate these effects on the perception of curvilinear heading, we manipulated object transparency in the manner described above, namely, as transparent, opaque, or black surfaces. The design of the present experiment was similar to Experiment 2 with the exception that in Experiment 3, we used only two moving objects.

Method

Participants. A total of 24 undergraduate students participated in partial fulfillment of a course requirement. There were 8 participants randomly assigned to each of the three transparency conditions. All had normal or corrected-to-normal vision.

Stimuli. In the previous experiments, given the extent and the location of the object in the environment, dots were generated randomly within that region and defined the object. The projected images of these dots were then displayed on the screen. In the present experiment, in addition to the dots defining the object, the overall contour of the object, especially for opaque and black objects, had to be drawn to yield the effect of dynamic occlusion of the background surface. To do so, we eliminated back surfaces (i.e., polygons) of an object that would be obscured from the observer's view by its front surfaces by back-face culling (Foley, van Dam, Feiner, & Hughes, 1997). The remaining surfaces (i.e., those facing the observer) were used to define the contour of each object and were drawn after the ground surface was drawn. When the images of the two objects overrode each other, the distant one had to be drawn first followed by the near one.

Still, rendering two objects whose image sizes varied significantly during the display increased the graphics load substantially. To ensure that each display was generated in real time, we ran the opaque and black objects conditions on a Silicon Graphics Indigo2 High Impact R10000 workstation, whereas the transparent condition was run on a Silicon Graphics Indigo2 R4400, the same machine used in Experiments 1 and 2. Displays were presented on the same monitor, a 19-in. (48.3-cm) screen refreshed at 60 frames/s, and viewed at a distance of 50 cm from a chin rest. Each display lasted about 2.5 s (150 frames).

As in Experiment 1, the observer's simulated velocity was controlled as tangential velocity and was held constant at 13.2 m/s. The two minivan size objects used in Experiment 2 were added to the flow field. The geometries of these objects' paths are depicted in Figure 9. At the beginning of each display, one object appeared on either side of the observer's path. We then varied the objects' path in three ways: In Object Path A–B, both objects moved parallel to the observer's path. In Object Path C, the outside object crossed the observer's path, whereas the inside object continued to move along its own path. In Object Path D, the inside object crossed the observer's future path, whereas the outside object continued to move along its own path.

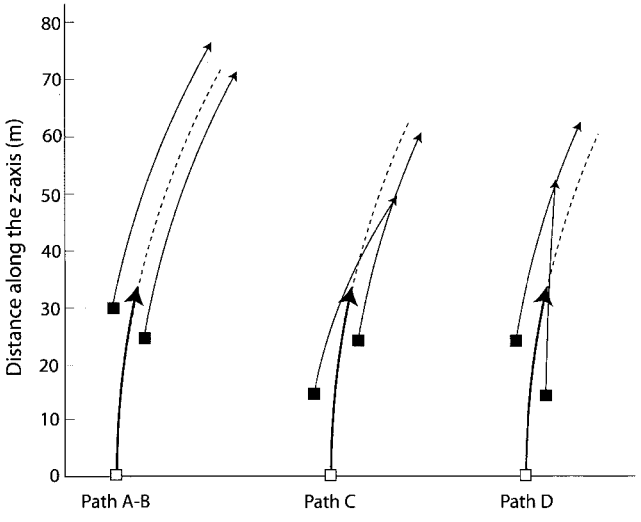

Figure 9. Plan view of the three object paths used in Experiment 3 for the $R = 160$ m condition. Initial positions for the observer and the objects are indicated by white and black squares, respectively. Final positions for the observer and the objects are indicated by arrowheads. Object paths are depicted by thin lines, and observer paths are depicted by thick lines. The projections of the observer paths are indicated by dotted lines.

Following the notation used to describe an object path in Experiment 2, the path of the outside object can be denoted in terms of aspect ratio for the observer's path as $(x + 4):(z + 4)$ and the path of the inside object as $(x - 3):(z - 3)$. At the beginning of each display, in Object Path A–B, the outside object lay 30 m, and the inside object lay 25 m in front of the observer. In Object Path C, the outside object lay 15 m and the inside object lay 25 m in front of the observer. In Object Path D, the outside object lay 25 m and the inside object lay 15 m in front of the observer. In Object Paths C and D, the near object was made to cross the observer's path by changing its aspect ratio by ± 0.04 m per frame (6 m for the duration of the trial; negative value for Object Path C and positive value for Object Path D).

Each object moved at two different speeds, relative to the observer. In Object Path A–B, the outside object moved either at an angular velocity of 2.6 degrees/s (0.05 radians/s) or 1.3 degrees/s (0.02 radians/s), and the inside object moved either at 2.8 degrees/s (0.05 radians/s) or 1.4 degrees/s (0.02 radians/s). In Object Path C, the outside object moved either at an angular velocity of 0.7 degrees/s (0.01 radians/s) or 0.35 degrees/s (0.006 radians/s), and the inside object moved either at 1.0 degrees/s (0.02 radians/s) or 0.5 degrees/s (0.01 radians/s). In Object Path D, the outside object moved either at an angular velocity of 1.0 degrees/s (0.02 radians/s) or 0.5 degrees/s (0.01 radians/s), whereas the inside object moved either at 0.7 degrees/s (0.01 radians/s) or 0.35 degrees/s (0.006 radians/s). The former pair of values for each object was used when the length of the *x*-axis of the observer's path was 160 m, whereas the latter pair was used when it was 320 m.

As in Experiment 2, the variations in observer's path and object's path changed the projected image size of each object. Table 2 shows how display image size for each of the two objects changed during a typical trial under different observer's path conditions.

Design. The curvature of the observer's path varied randomly among ± 160:320 m, ± 320:160 m, ± 160:160 m, and ± 320:320 m (positive values correspond to a right-hand turn and negative values correspond to a left-hand turn). Heading angle varied randomly among values of $\pm 0.5°$, $\pm 1°$, $\pm 2°$, and $\pm 4°$. This yielded a 3 (transparency) $\times$ 3 (object path) $\times$ 4 (curvature) $\times$ 2 (turn direction) $\times$ 4 (heading angle) $\times$ 2 (target location) mixed design with 192 trials. All variables were controlled within subjects, except transparency, which was controlled between subjects.

Procedure. As in the previous experiments, a short practice session preceded the main experiment. The eight practice trials were created by crossing four circular paths ($R = \pm 240$ m or ± 480 m) with two heading angles ($\pm 5°$). The practice trials contained two moving objects and followed Object Path A. Participants saw only displays using the transparency condition they would see in the experimental condition. As in previous experiments, feedback was provided during the practice session but was not given during the experiment.

In the present experiment, object path varied in three different ways, rather than in four ways as in the previous experiments. We found that there were too few repetitions to allow us to determine a heading threshold for each curvature of the observer's path. In the black object condition, especially in the 320:160 m curvature condition (i.e., the observer's path with the largest curvature), 4 participants failed to reach threshold. Hence, heading thresholds for curvature were excluded from analyses, and only thresholds for object paths were presented.

Results and Discussion

The percentage of correct responses for each condition of the curvature of the observer's path is presented in Figure 10A and for each condition of object path in Figure 10B, both as a function of the transparency of the object. Overall, the percentage of correct responses was 70%. For analysis, the results were collapsed over

Table 2
Maximum and Minimum Image Sizes of Each Moving Object by Curvature of Observer's Path in Experiments 3 and 4

		Experiment 3		Experiment 4	
Observer's path (m)	Object	Max. (deg)	Min. (deg)	Max. (deg)	Min. (deg)
160:320	A	3 × 2	2 × 2	6 × 4	1 × 1
	B	4 × 4	3 × 3	16 × 11	1 × 1
320:160	A	16 × 12	3 × 9	14 × 10	4 × 3
	B	6 × 7	5 × 9	18 × 16	4 × 4
160:160	A	10 × 6	5 × 5	11 × 9	3 × 2
	B	4 × 4	3 × 3	9 × 8	2 × 2
320:320	A	9 × 6	2 × 1	9 × 6	2 × 1
	B	5 × 4	4 × 3	16 × 12	2 × 2

Note. Max. = maximum; Min. = minimum; deg = degrees.

the signs of turn direction and target location and entered into a 3 (transparency) × 3 (object path) × 4 (curvature) × 4 (heading angle) mixed-design ANOVA. The effects of heading angle, $F(3, 63) = 142.72$, $p < .01$, and curvature, $F(3, 63) = 7.80$, $p < .01$, were reliable, as was the interaction between object path and curvature, $F(6, 126) = 5.03$, $p < .01$. The fourth-order interaction involving transparency, object path, aspect, and heading angle was also significant. The effect of curvature seen here is consistent with previous findings (e.g., Kim & Turvey, 1998) as well as the results of previous experiments. With respect to the Object Path × Curvature interaction, a simple effects analysis revealed significance of curvature at Object Path A–B, $F(3, 63) = 3.14$, $p < .05$; and Object Path D, $F(3, 63) = 12.83$, $p < .01$. The same analysis also revealed significance of object path at the 320:160 condition, $F(2, 42) = 9.07$, $p < .01$, but not at other curvature conditions. Performance in the 320:160 Object Path D condition was worse (59%) than in any other conditions. Indeed, inspection of Figure 11 reveals that the interaction between curvature and object path is largely due to participants' poor performance in this condition.

Transparency had a negligible effect on heading accuracy, $F(2, 21) = 2.16$, $p > .05$. Overall performance in each condition of transparency was 68% for transparent objects, 73% for opaque objects, and 69% for black objects, respectively. Performance for the two transparent objects was comparable to that observed in Experiment 2 with three objects. Moreover, except for the fourth-order interaction reported above, there were no significant interactions involving transparency.

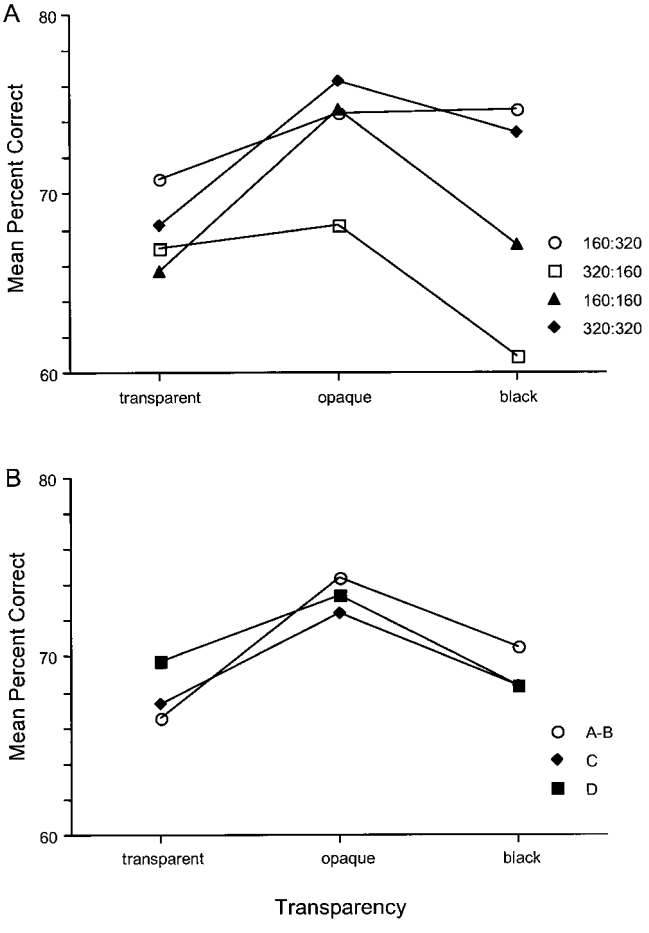

Figure 10. Percentages of correct responses in Experiment 3 for each condition of curvature of the observer's path (A) and for each object path (B) as a function of object transparency.

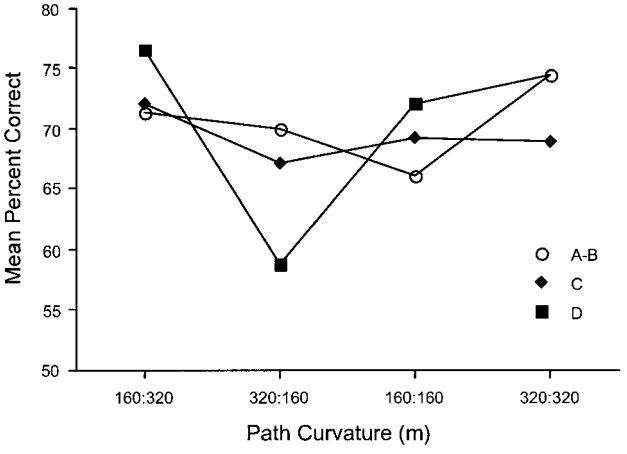

Figure 11. Percentages of correct responses in Experiment 3 for the three object paths as a function of the curvature of the observer's path.

Thresholds for the three object paths are presented as a function of object transparency in Figure 12A. The overall mean heading threshold was 2.3°. An ANOVA on thresholds with transparency and object path as independent variables further confirmed the results of the preceding analysis. Neither the two main effects nor their interaction was reliable. Taken together, the results of the two foregoing analyses on heading accuracy were not different from the previous findings and showed a comparable level of accuracy. In brief, different degrees of object transparency had minimal effects on accuracy of perceived heading.

For each condition of transparency, the percentages of outside responses were 39% for transparent objects, 51% for opaque objects, and 56% for blank objects, respectively (Figure 12B). Of these, an inside tendency was significant for transparent objects, $t(7) = -4.83$, $p < .01$. To further examine the contrasting pattern of heading bias, we performed a 3 (transparency) × 3 (object path) × 4 (curvature) mixed-design ANOVA on percentages of outside responses. The results showed significant main effects of object path, $F(2, 42) = 22.97$, $p < .01$; and curvature, $F(3, 63) = 72.99$, $p < .01$. However, the main effect of transparency was not significant, $F(2, 21) = 2.67$, $p > .05$; but it was qualified by a significant interaction with object path, $F(4, 42) = 4.22$, $p < .01$.

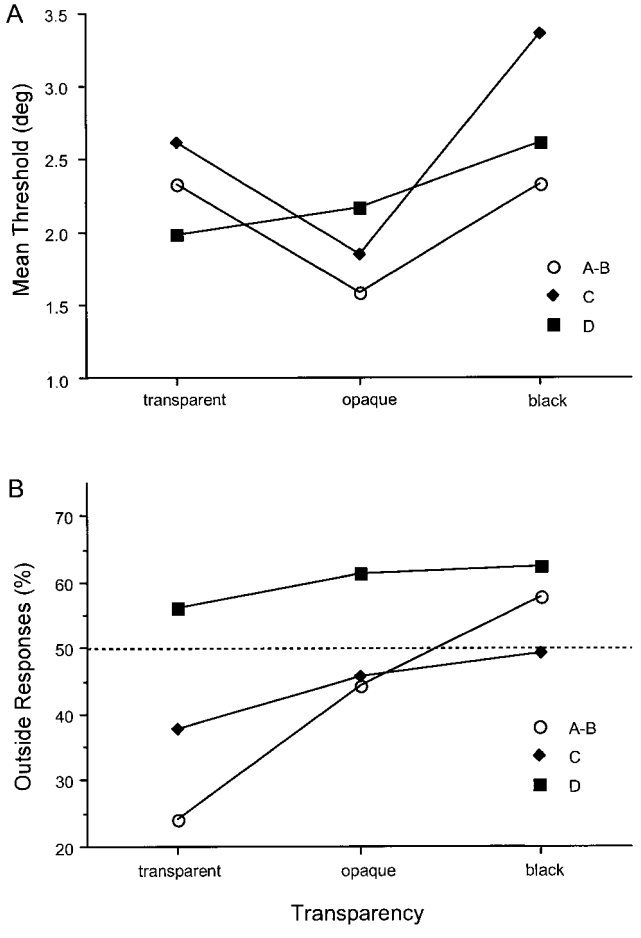

Figure 12. Mean heading thresholds (A) and percentages of outside responses (B) in Experiment 3 for the three object paths as a function of object transparency. The horizontal reference line at 50% (in B) indicates no heading bias. deg = degrees.

The main effect of curvature largely replicates the pattern observed in previous experiments. That is, across all conditions of transparency, outside biases for the observer's paths of 160:320, 320:160, 160:160, and 320:320 were 39%, 65%, 48%, and 42%, respectively, but only 160:320 and 320:320 conditions were significantly different from 50%, $t(23) = -3.53$, $p < .01$, and $t(23) = -2.44$, $p < .05$, the same conditions that induced inside biases in Experiment 2. With respect to the main effect of object path, participants showed inside preferences for Object Path A–B (M = 42%) and C (M = 44%) but outside tendency for Object Path D (M = 60%). Of these, only Object Path D reached significance, $t(23) = 3.61$, $p < .01$.

With respect to the Transparency × Object Path interaction, a simple effects analysis showed that the effect of object path was significant at all conditions of transparency, whereas the effect of transparency was significant only at Object Path A–B, $F(2, 21) = 7.95$, $p < .01$, but not at Object Path C or D ($F < 1$). It was clearly the different bias pattern at Object Path A–B across the three transparency conditions that induced this interaction. It appears that the inside tendency observed in analogous conditions in Experiment 2 (i.e., Object Paths A and B) was further exaggerated in Experiment 3 (percentage of outside responses = 24%), $t(7) = -10.40$, $p < .01$. Recall that percentages of outside responses were 34% and 38% for Object Paths A and B, respectively, in Experiment 2, with neither reaching statistical significance. Similar tendencies were absent for opaque and black objects.

In summary, the effect of transparency was virtually negligible not only on the accuracy of perceived heading but also on bias except for some anomalous inside tendency with transparent objects especially at Object Path A–B. The results of the present study support the hypothesis that the visual system is able to cope with moving objects and does not pool together all velocity vectors, including those corresponding to the moving objects. In Experiment 4, we continued to examine the effect of transparency under conditions in which the objects approached the observer, rather than retreated as in Experiments 1, 2, and 3.

Experiment 4: Approaching Objects

In the displays used in Warren and Saunders's (1995) study, the object always approached the observer. In most of the displays used by Royden and Hildreth (1996), the object did not move in depth relative to the observer. Both studies reported a bias, but in opposite directions. Moreover, Royden and Hildreth found considerable variation in direction of bias among participants. Judgments of some participants were biased in the direction of the object's motion, and judgments of other participants were biased in the direction opposite the object's motion. These divergent results suggest a need for further examination of the relationship between object motion in depth and bias direction. Because of the different types of observer movement examined, a direct comparison between the two preceding studies and the present study is difficult. Nonetheless, to examine the effect of object motion in depth on perceived heading, we reversed the direction of object motion in Experiment 4 so that the object approached the observer.

Method

Participants. A total of 24 undergraduate students participated in partial fulfillment of a course requirement. There were 8 participants randomly assigned to each of the three transparency conditions. All had normal or corrected-to-normal vision.

Stimuli. The same display used in Experiment 3 was used in Experiment 4 with two exceptions. Although the geometries for object path and simulated speed for observer movement used in Experiment 4 were identical to those used in Experiment 3, because the objects approached rather than retreated from the observer, their starting locations were different (see Figure 13). In Object Path A–B, the outside object was 70 m and the inside object was 65 m in front of the observer. In Object Path C, the outside object was 65 m and the inside object was 55 m in front of the observer. In Object Path D, the outside object was 55 m and the inside object was 65 m in front of the observer. As in Experiment 3, the near object in Object Paths C and D crossed the observer's path by changing its aspect ratio by ±0.04 m per frame (6 m over the duration of the trial, with the negative value for Object Path C and the positive value for Object Path D).

In Experiment 4, objects moved at a tangential velocity of 6.2 m/s (or 14.9 mph), regardless of the curvature of the observer's path. Because objects approached the observer, the relative speed was 19.8 m/s (or 44.6 mph).

The change in image size of each object over a typical trial is shown in Table 2 for each observer's path condition. As both objects approached the observer, their image sizes expanded considerably. In Object Paths C and D, wherein one object crossed the observer's path to the same side as the other object, the closer object typically occluded the more distant object.

Design. The same design used in Experiment 3 was used in Experiment 4, that is, a 3 (transparency) × 3 (object path) × 4 (curvature) × 2 (turn direction) × 4 (heading angle) × 2 (target location) mixed design with 192 trials. As in Experiment 3, the curvature of the observer's path varied randomly among ±160:320 m, ±320:160 m, ±160:160 m, and ±320:320 m. Heading angle also varied randomly among values of ±0.5°, ±1°, ±2°, and ±4°. As in Experiment 3, all variables were controlled within subjects, except transparency, which was between subjects.

Procedure. The procedure adopted in Experiment 4 was identical to that in Experiment 3. That is, a short practice session preceded the main experiment. In the practice session, participants saw only displays using the same transparency condition that they would see in the experimental condition. Feedback was provided during the practice session but was not given during the experiment.

As in Experiment 3, 3 participants (2 in the transparent condition and 1 in the opaque condition) failed to reach the 75% correct criterion in one of the curvature conditions for all four heading angles. Consequently, heading thresholds for curvature were excluded, and only thresholds for object paths were analyzed.

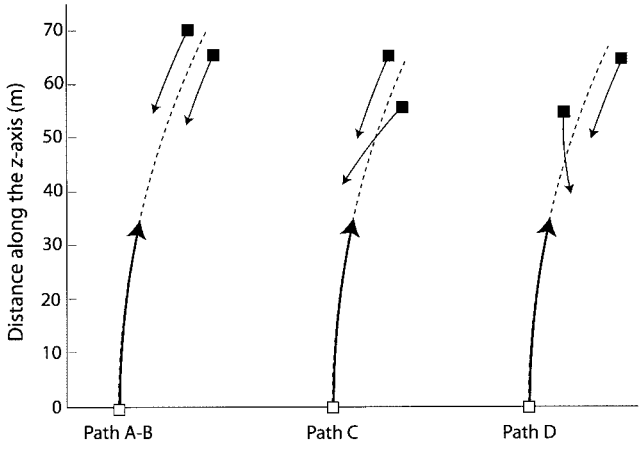

Figure 13. Plan view of the three object paths used in Experiment 4 for the $R = 160$ m condition. Initial positions for the observer and the objects are indicated by white and black squares, respectively. Final positions for the observer and the objects are indicated by arrowheads. Object paths are depicted by thin lines, and observer paths are depicted by thick lines. The projections of the observer paths are indicated by dotted lines.

Results and Discussion

The percentage of correct responses for each condition of the curvature of the observer's path is presented in Figure 14A and for each condition of the object's path in Figure 14B, both as a function of the transparency of the object. For analysis, we collapsed the results over the signs of turn direction and target location and entered into a 3 (transparency) × 3 (object path) × 4 (curvature) × 4 (heading angle) mixed-design ANOVA. The effects of heading angle, $F(3, 63) = 140.22$, $p < .01$, and curvature, $F(3, 63) = 18.52$, $p < .01$, were reliable, replicating the results of the three previous experiments. None of the other main effects or interactions were significant. As in Experiment 3, the effect of transparency of perceived heading accuracy was negligible ($F < 1$). Overall performance by transparency condition was 75% for transparent objects, 71% for opaque objects, and 72% for black objects.

An ANOVA on thresholds with transparency and object path as independent variables revealed no significant main effects or interactions. The overall mean heading threshold was 2.1° (Figure 15A). In short, despite the fact that objects approached rather than retreated from the observer in Experiment 4, different object paths and different types of transparency did not appear to affect heading judgments, consistent with the three previous experiments.

The percentages of outside responses for each condition of transparency were 49% for transparent objects, 43% for opaque objects, and 56% for black objects, respectively (Figure 15B). None reached statistical significance. Recall that participants in the transparent object condition in Experiment 3 exhibited an inside bias. Following Experiment 3, a 3 (transparency) × 3 (object path) × 4 (curvature) mixed-design ANOVA was performed on percentages of outside responses. The main effects of object path, $F(2, 42) = 5.12$, $p < .01$, and curvature, $F(3, 63) = 106.75$, $p < .01$, were significant, but transparency, $F(2, 21) = 2.31$, $p > .05$, was not, replicating the results of Experiment 3. Unlike Experiment 3, however, the Object Path × Transparency interaction, $F(4, 42) = 1.26$, $p > .05$, was not significant.

The main effect of curvature was consistent with the results observed in previous experiments, that is, outside bias at smaller curvature (i.e., 320:160; $M = 69\%$), $t(23) = 6.12$, $p < .01$, and inside bias at larger curvature (i.e., 160:320; $M = 38\%$), $t(23) = -6.14$, $p < .01$; for 320:320 ($M = 41\%$), $t(23) = -3.49$, $p < .01$. The percentage of outside responses at each condition of object path was 46% for A–B, 52% for C, and 49% for D, of which none differed from 50%. Hence, despite the significant effect of object path, the response pattern at each condition did not exhibit any bias. More important, the insignificance of transparency in conjunction with the absence of the Object Path × Transparency interaction further corroborates the suspicion that the apparent inside tendency with transparent objects at Object Path A–B observed in Experiment 3 was indeed an anomaly.

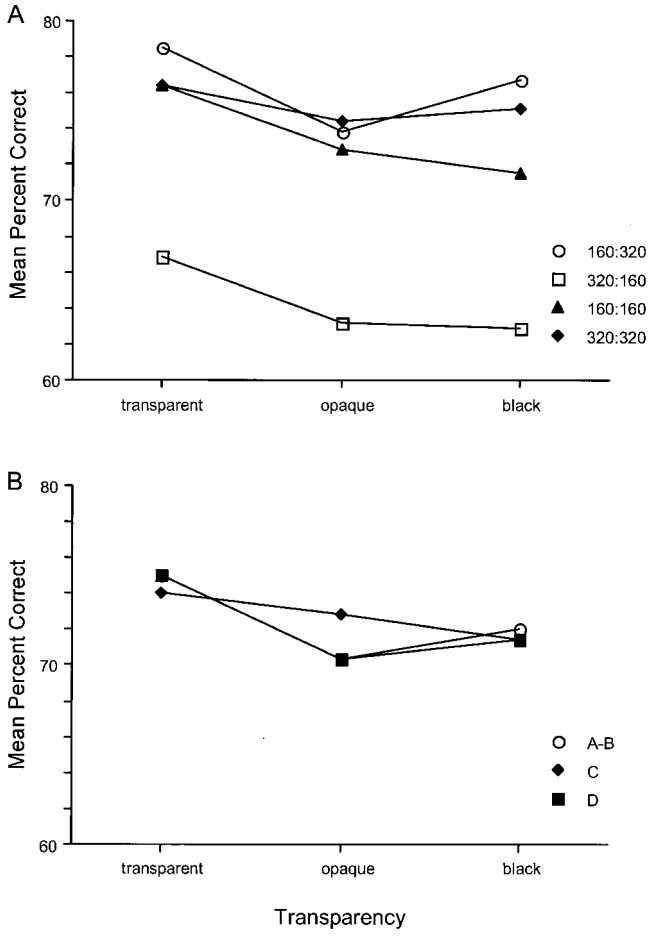

Figure 14. Percentages of correct responses in Experiment 4 for each condition of curvature of the observer's path (A) and for each object path (B) as a function of object transparency.

It appears that the parameter specifically manipulated in Experiment 4 (i.e., direction of object motion) had a minimal effect on heading judgments, as the results largely replicated those of Experiment 3. To further examine its effect, however, we combined the results in Experiments 3 and 4 of percentages of correct responses and entered them into a mixed-design ANOVA with motion direction, transparency, object path, curvature, and heading angle as independent variables. The ANOVA showed the main effects of curvature, $F(3, 132) = 24.96$, $p < .01$; and heading angle, $F(3, 132) = 289.63$, $p < .01$; an Object Path $\times$ Curvature interaction, $F(6, 264) = 2.44$, $p < .05$; a third-order interaction involving object path, curvature, and motion direction, $F(6, 264) = 3.60$, $p < .01$; and a fourth-order interaction involving object path, curvature, heading angle, and transparency, $F(36, 792) = 1.70$, $p < .01$. It is important to note that insignificance of motion direction, $F(1, 44) = 1.89$, $p > .05$, further corroborates the suspicion that direction of object motion had minimal effect on perceived curvilinear heading. Also notable are the reliable main effects of heading angle and curvature and unreliable main effect of transparency, a pattern consistent with previous experiments (although transparency figured in the four-way interaction). In summary, in Experiment 4, wherein objects approached the observer, performance remained quite accurate with an overall heading threshold of 2.1° and largely intact from any bias.

General Discussion

In the present study, we set out to examine the effect of moving objects on heading perception while negotiating a curved path, focusing on five aspects of such a situation. First, the simulated self-motion was varied in terms of the type of path, either circular or elliptical, and degree of curvature, ranging from moderate to extreme. Second, objects either moved in parallel with the observer, crossed the observer's future path from inside to outside, or crossed from outside to inside. Third, the number of objects moving with the observer varied from one to a maximum of three. Fourth, following Warren and Saunders's (1995) study, objects were depicted as either transparent, opaque, or black. Fifth, objects either approached the observer or retreated in depth relative to the observer.

Performance was quite accurate, despite the various perturbations introduced to the flow field. Overall heading thresholds were

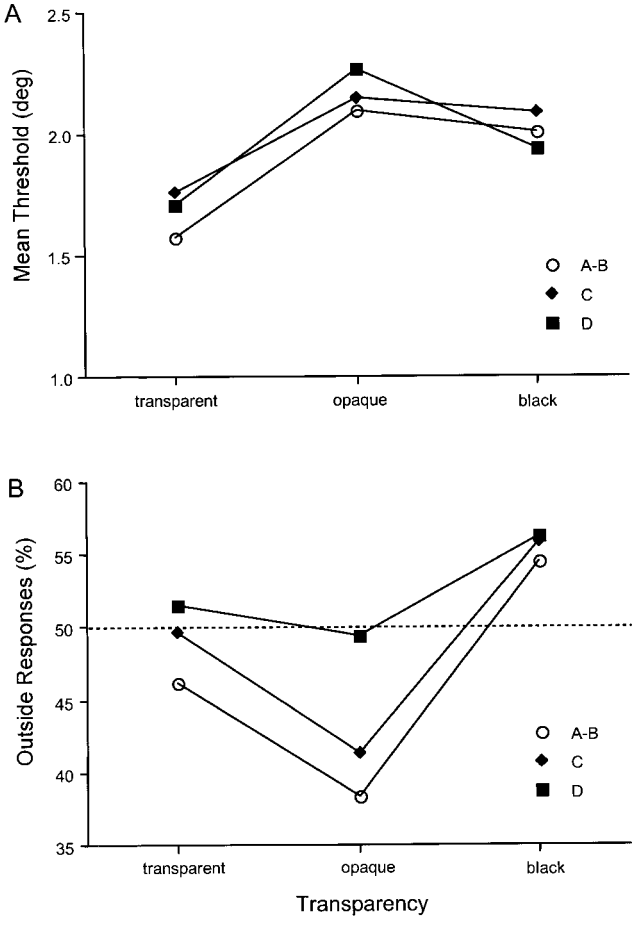

Figure 15. Mean heading thresholds (A) and percentages of outside responses (B) in Experiment 4 for the three object paths as a function of object transparency. The horizontal reference line at 50% (in B) indicates no heading bias. deg = degrees.

on the order of 2.2° for one retreating object (Experiment 1), 2.3° for three retreating objects (Experiment 2), 2.3° for two retreating objects (Experiment 3), and 2.1° for two approaching objects (Experiment 4), all well within the range required for observer movement at the simulated speed (Cutting, 1986). Of particular interest, however, is the consistency of performance across all four experiments. This consistency was observed over different numbers of objects in the flow field, different object paths relative to the observer's path, and different types of transparency of the objects' surfaces. The effects of object path on accuracy across all four experiments were virtually negligible, as were the effects of transparency in Experiments 3 and 4. Moreover, the absence of a particular pattern of bias further corroborates these results. Participants' judgments were influenced as a function of curvature of the observer's path, but the response pattern was consistent with the results of the previous studies without moving objects (Kim & Turvey, 1998; Warren, Mestre, et al., 1991), that is, inside bias for observer paths of small curvature and outside bias for observer paths of larger curvature. Taken together, there is virtually no evidence that indicates that the presence of moving objects affected human observers' capacity to perceive direction of curvilinear heading. In short, human observers were equally accurate in perceiving curvilinear heading with or without moving objects in their field of view.

Computational Models Revisited

We have focused on two computational models of the visual system, Warren and Saunders's (1995) template model and Hildreth's (1992; see also Royden & Hildreth, 1996, 1999) motion parallax model, for their ability to handle noise induced by moving objects. Both models demonstrated accurate self-motion estimation in the presence of a moving object, and their robust performance was achieved either by exploiting the redundancy of the flow field (Warren & Saunders, 1995) or by administering a consistency check that filters out the noise in the image plane (Hildreth, 1992).

First, consider the implications of the present findings for the Warren and Saunders's (1995) model. Because this model works by pooling velocity vectors over the entire visual field, one would expect inaccuracies and biases in heading estimates under certain conditions. Moreover, objects that cross the observer's future path should influence judgments more, because velocity vectors in the center of the visual field are weighted more heavily. In general, one would expect different biases, in terms of magnitude and direction, under different conditions of object path, number of objects, and object transparency. Insofar as these manipulations had no effect on heading accuracy, the results of the present study provide strong evidence against models that cope with moving objects by pooling velocity vectors over the entire visual field.

Instead, the results suggest that observers were able to successfully distinguish between the moving objects and the stationary background and that heading judgments were based on the optical flow corresponding to the stationary background. The finding that heading judgments were basically unaffected by moving objects is consistent with the Hildreth (1992) model, which segments moving objects prior to estimating heading. Nonetheless, the Hildreth model may not account for all of the present data. Because this model uses relative motion to segment moving objects, one would expect accurate performance in the presence of black and transparent objects. To the extent that less relative motion impedes the segmentation of moving objects, performance in the opaque object condition may be worse, because it contains less relative motion (Warren & Saunders, 1995). In the present study, there were no significant main effects of object transparency, and differences in means often suggested that performance in the opaque and black conditions was actually more accurate, albeit not significantly. At the very least then, it is unclear whether the Hildreth model could account for performance in all three conditions of object transparency.

Of course, it is possible that observers used relative motion in the manner described by Hildreth (1992) to segment transparent objects and another source of information to segment black and opaque objects. As we pointed out in the introduction, however, the Hildreth model was designed to identify instantaneous heading rather than the future path. Although the model is quite capable of segmenting moving objects during curvilinear observer movement, the very same process that recovers the radial pattern of flow necessary for segmentation also eliminates the rotational component of flow that is necessary to identify the future path. Hence, this computational step would have to be undone once the moving objects were segmented to estimate the future path. Although, in principle, the visual system may perform these steps sequentially, we argue that a more parsimonious account should be favored. In the next section, we offer an alternative account based on the idea that moving objects break the continuity of vector directions that must be preserved for the optic array to contain information about one's direction of self-motion.

Continuity of Vector Directions

For land-based animals, locomotion is generally restricted to the ground surface, which is typically rigid and stationary. In an open, uncluttered environment, all surfaces are projected to the point of observation, and a one-to-one correspondence between environmental elements and their optical counterparts is preserved in the optical transformation resulting from observer locomotion. Accordingly, locomotion of the observer over a ground surface is specified by a global transformation of the optic array (Gibson, 1954, 1968), which is characterized by a smooth, continuous optical motion. That is, movement of the observer over a ground plane produces a transformation of the optic array that contains no breaks or discontinuities in the directions of neighboring velocity vectors.[1] Moreover, this holds for both linear and curvilinear observer movement.

In contrast, movement of an observer through an environment containing moving objects produces local transformations of the

[1] Warren, Blackwell, et al. (1991) demonstrated that linear and circular heading judgments were unaffected by noise in image vector magnitudes but deteriorated when noise was added to vector directions. On the basis of these results, the authors concluded that the information for self-motion is contained in the directions, not the magnitudes, of image vectors. Thus, discontinuities in image vector magnitudes are of no consequence to the mechanisms involved in perception of heading. The more important factor is that for self-motion over a ground plane, there are no discontinuities in vector directions (see also Kim & Turvey, 1998, for a similar finding but with flow fields engendered from translation along a curved path).

optic array characterized by discontinuities in the directions of neighboring velocity vectors. That is, an image vector corresponding to a moving object will point in a different direction than an image vector in the same visual direction corresponding to the stationary background. Thus, one might conclude that information about self-motion is contained in global transformations of the optic array that preserve the continuity of vector directions. Because moving objects break this continuity, regions containing moving objects may not provide information about the movement of the observer.

Breaks in the continuity of vector directions, however, are not specific to moving objects. During curvilinear observer movement through an environment containing stationary objects resting on the ground surface, the continuity of vector directions is also broken in regions corresponding to the stationary objects. The most extreme example is curvilinear movement through a rigid 3-D cloud (Warren, Mestre, et al., 1991), in which discontinuities in vector directions exist in every direction. Unlike linear movement, two image vectors corresponding to points in the same visual direction at different depths may point in different directions. Thus, whereas vector fields with continuous vector directions guarantee a rigid environment that provides reliable information about self-motion, vector fields with discontinuities do not guarantee a rigid environment and may or may not reliably specify direction of self-motion. As long as stationary or moving objects do not occlude the entire ground surface, at least some portion of the visual field will provide reliable information about self-motion. In such situations, it is reasonable to believe that observers will use the reliable information to the extent that it is available and disregard the regions of the visual field that contain discontinuities of vector directions, because they do not reliably specify direction of self-motion.

How might this principle account for the present finding that performance was unaffected in all three conditions of object transparency? In the black condition, moving objects produced no discontinuities in vector directions and left much of the ground surface unoccluded. Hence, performance was unaffected by the presence of black objects. In the transparent condition, regions of the visual field with moving objects contained numerous violations of the continuity among neighboring vector directions. Because much of the ground surface was unoccupied by moving objects, however, reliable information was still available. Hence, regions corresponding to transparent moving objects did not influence perception, because observers could afford to disregard these regions. In the opaque condition, although discontinuities of vector directions could be found along the contours of moving objects, vector directions were continuous within the regions of the visual field corresponding to the moving objects. How might the visual system determine which region of the visual field corresponds to the moving object and which corresponds to the stationary background? First, moving objects will tend to produce local transformations of the optic array that can be distinguished from global transformations corresponding to observer movement. Thus, as long as a moving object does not occupy the majority of the visual field, it can be identified as such and disregarded. Second, the stationary background typically corresponds to the surface in the scene at the greatest depth. In natural environments, which typically contain opaque surfaces, information about the ordinal relations among surfaces in the scene is provided by dynamic occlusion. Thus, even if a moving object does occupy the majority of the visual field, the stationary background can still be identified by dynamic occlusion. In summary, the finding that performance was equivalent in all three conditions of object transparency is consistent with the principle that observers use the reliable information when it is available and disregard regions of the visual field that contain breaks in the continuity of vector directions.

This is not to say that the presence of moving objects will never impair heading perception. One would certainly not be surprised to find that many moving objects that occupy a large portion of the visual field could result in degraded performance. However, such degradation would not be attributable to the large number of image vectors corresponding to moving objects. Rather, the failure of perception would result from the absence of reliable information about one's direction of self-motion due to occlusion of the stationary ground surface by opaque moving objects or breaks in the continuity of vector directions across large regions of the visual field by transparent moving objects. In the absence of reliable information, observers would be forced to use the information from regions of the vector field that contain breaks in the continuity of vector directions. When these discontinuities result from moving objects, performance would degrade. Under conditions in which those discontinuities result from stationary objects, perception would be unaffected. This is consistent with the findings of Warren, Mestre, et al. (1991), who demonstrated that observers can accurately judge their future path during curvilinear movement through a rigid 3-D cloud of dots. According to the present account, participants were forced to use the information in the regions containing discontinuities, because reliable information about self-motion was unavailable. Despite the presence of discontinuities throughout the visual field, their judgments were accurate in this particular case, because the environment was rigid and did not contain moving objects. Had moving objects been present, one would expect judgments of heading during movement through a 3-D cloud to degrade. This leads to a testable prediction. On the basis of the present argument, transparent moving objects should affect curvilinear heading judgments during movement through a 3-D cloud of dots but not during movement over a ground surface.

If moving objects destroy the information, rather than provide misinformation about self-motion, then why did both Warren and Saunders (1995) and Royden and Hildreth (1996) observe biases in their experiments? We hasten to point out that these biases were quite small, restricted to conditions in which the moving object crossed the FOE, and in some conditions varied considerably from observer to observer in both magnitude and direction. As Royden and Hildreth surmised, such individual differences suggest that there is no single mechanism for coping with moving objects that crossed the FOE. Rather, it appears that different observers learned to use different strategies. Given the small and inconsistent nature of this bias, we feel that too much emphasis has been placed on accounting for biases and not enough on the more robust finding that all observers are able to perceive heading accurately under these demanding conditions. Although a better understanding of these biases may reveal something important about the mechanisms that underlie heading perception, a better understanding of the overall accuracy may be equally revealing.

Eye Movement Strategies

In none of the previous models for coping with moving objects do eye movements play a special role. It is quite possible that the visual system's ability to disregard moving objects is based, in part, on particular search strategies of eye movements that are used in the presence of moving objects. Nonetheless, the main objective of this study was to add to the existing literature on heading perception during curvilinear movement and in the presence of moving objects. Because free eye movements have primarily been used in previous studies in both areas of research, we opted to allow free eye movements in the present experiments. Future research should consider the possible role for eye movements in the search for information about self-motion in the presence of moving objects.[2]

Summary and Conclusion

The present study clearly demonstrates that observers are capable of disregarding moving objects to make accurate, unbiased estimates of heading. These findings are inconsistent with models of heading perception that cope with moving objects by pooling velocity vectors over the entire visual field (e.g., Warren & Saunders, 1995) and favor models that segment moving objects prior to estimating heading (e.g., Hildreth, 1992). To segment moving objects, however, the Hildreth model requires a radially expanding pattern of optic flow that does not contain a rotational component. Although this model is capable of extracting a radially expanding pattern from optical flow induced by curvilinear observer movement, the rotational component that is removed by this operation is required to estimate the observer's curvilinear movement (i.e., the future path). The fact that observers were able to successfully estimate their future curvilinear path in the presence of moving objects suggests that they make use of such information. We suggest that, alternatively, information about self-motion is contained in transformations of the optic array that preserve the continuity of vector directions. Because moving objects break this continuity, regions of the visual field containing moving objects do not provide information about self-motion. Hence, the visual system can disregard these regions and estimate self-motion on the basis of the optical motion of the stationary background. In situations in which the surfaces of moving objects are opaque, the stationary background generally corresponds to the surface with the greatest depth, which is specified by dynamic occlusion. This principle, which applies to both linear and curvilinear observer movement, provides a parsimonious account of the success with which observers in the present study were able to perceive their future path in the presence of moving objects.

[2] However, see Kim and Turvey (1999) or Wann and Swapp (2000) for a possible role that eye movements play in extracting the requisite information for self-motion from the flow field.

References

Andersen, G. J., & Braunstein, M. L. (1985). Induced self-motion from optic flow in the central visual field. *Journal of Experimental Psychology: Human Perception and Performance, 11,* 122–132.

Ballard, D. H., & Kimball, O. A. (1983). Rigid body motion from depth and optical flow. *Computer Vision, Graphics, and Image Processing, 22,* 95–115.

Bruss, A. R., & Horn, B. K. P. (1983). Passive navigation. *Computer Vision, Graphics, and Image Processing, 21,* 3–20.

Cutting, J. E. (1986). *Perception with an eye for motion*. Cambridge, MA: MIT Press.

Cutting, J. E., Springer, K., Braren, P. A., & Johnson, S. H. (1992). Wayfinding on foot from information in retinal, not optical, flow. *Journal of Experimental Psychology: General, 121,* 41–72.

Cutting, J. E., Vishton, P. M., & Braren, P. A. (1995). How we avoid collisions with stationary and moving obstacles. *Psychological Review, 102,* 627–651.

Foley, J. D., van Dam, A., Feiner, S. K., & Hughes, J. F. (1997). *Computer graphics: Principles and practice*. Reading, MA: Addison-Wesley.

Gibson, J. J. (1954). The visual perception of objective motion and subjective movement. *Psychological Review, 61,* 304–314.

Gibson, J. J. (1966). *The senses considered as perceptual systems*. Boston: Houghton Mifflin.

Gibson, J. J. (1968). What gives rise to the perception of motion? *Psychological Review, 75,* 335–346.

Gibson, J. J. (1986). *The ecological approach to visual perception*. Hillsdale, NJ: Erlbaum. (Original work published 1979)

Gibson, J. J., Kaplan, G. A., Reynolds, H., & Wheeler, K. (1969). The change from visible to invisible: A study of optical transitions. *Perception & Psychophysics, 5,* 113–116.

Hatsopoulos, N. G., & Warren, W. H. (1990). Visual navigation with a neural network. *Neural Networks, 4,* 303–317.

Heeger, D. J., & Jepson, A. D. (1990). Visual perception of three-dimensional motion. *Neural Computation, 2,* 129–139.

Heeger, D. J., & Jepson, A. D. (1992). Subspace methods for recovering rigid motion: I. Algorithm and implementation. *International Journal of Computer Vision, 7,* 95–117.

Hildreth, E. C. (1992). Recovering heading for visually-guided navigation. *Vision Research, 32,* 1177–1192.

Kaplan, G. A. (1969). Kinetic disruption of optical texture: The perception of depth at an edge. *Perception & Psychophysics, 6,* 193–198.

Kim, N.-G., Fajen, B. R., & Turvey, M. T. (2000). Perceiving circular heading in noncanonical flow fields. *Journal of Experimental Psychology: Human Perception and Performance, 26,* 31–56.

Kim, N.-G., & Turvey, M. T. (1998). Visually perceiving direction of heading on circular and elliptical paths. *Journal of Experimental Psychology: Human Perception and Performance, 24,* 1690–1704.

Kim, N.-G., & Turvey, M. T. (1999). Eye movements and a rule for perceiving direction of heading. *Ecological Psychology, 11,* 233–248.

Longuet-Higgins, H. C., & Prazdny, K. (1980). The interpretation of moving retinal images. *Proceedings of the Royal Society of London, Series B, 208,* 385–397.

Perrone, J. A. (1992). Model for the computation of self-motion in biological systems. *Journal of the Optical Society of America A, 9,* 177–194.

Perrone, J. A., & Stone, L. S. (1994). A model of self-motion estimation within primate extrastriate visual cortex. *Vision Research, 34,* 2917–2938.

Prazdny, K. (1981). Determining the instantaneous direction of motion from optical flow generated by a curvilinearly moving observer. *Computer Graphics and Image Processing, 17,* 238–258.

Rieger, J. H., & Lawton, D. T. (1985). Processing differential image motion. *Journal of the Optical Society of America A, 2,* 354–360.

Royden, C. S., Crowell, J. A., & Banks, M. S. (1994). Estimating heading during eye movements. *Vision Research, 34,* 3197–3214.

Royden, C. S., & Hildreth, E. C. (1996). Human heading judgments in the presence of moving objects. *Perception & Psychophysics, 58,* 836–856.

Royden, C. S., & Hildreth, E. C. (1999). Differential effects of shared

attention on perception of heading and 3-D object motion. *Perception & Psychophysics, 61,* 120–133.

van den Berg, A. V. (1992). Robustness of perception of heading from optic flow. *Vision Research, 32,* 1285–1296.

Wann, J. P., & Swapp, D. K. (2000). Why you should look where you are going. *Nature Neuroscience, 3,* 647–648.

Warren, W. H (1995). Self-motion: Visual perception and visual control. In W. Epstein & S. Rogers (Eds.), *Handbook of perception and cognition: Vol. 5. Perception of space and motion* (pp. 263–325). San Diego, CA: Academic Press.

Warren, W. H., Blackwell, A. W., Kurtz, K. J., Hatsopoulos, N. G., & Kalish, M. L. (1991). On the sufficiency of the velocity field for perception of heading. *Biological Cybernetics, 65,* 311–320.

Warren, W. H., & Hannon, D. J. (1990). Eye movements and optical flow. *Journal of the Optical Society of America A, 7,* 160–169.

Warren, W. H., & Kurtz, K. J. (1992). The role of central and peripheral vision in perceiving the direction of self-motion. *Perception & Psychophysics, 51,* 443–454.

Warren, W. H., Mestre, D. R., Blackwell, A. W., & Morris, M. W. (1991). Perception of circular heading from optical flow. *Journal of Experimental Psychology: Human Perception and Performance, 17,* 28–43.

Warren, W. H., Morris, M. W., & Kalish, M. (1988). Perception of translational heading from optical flow. *Journal of Experimental Psychology: Human Perception and Performance, 14,* 644–660.

Warren, W. H., & Saunders, J. A. (1995). Perceiving heading in the presence of moving objects. *Perception, 24,* 315–331.

Received March 27, 2000
Revision received November 15, 2001
Accepted February 19, 2002 ■